Memories - Materials, Devices, Circuits and Systems 4 (2023) 100060

Contents lists available at ScienceDirect

Memories - Materials, Devices, Circuits and Systems

journal homepage: www.elsevier.com/locate/memori

Survey on compressed sensing over the past two decades

Sherif Hosny [a,b], M. Watheq El-Kharashi [a,c,*], Amr T. Abdel-Hamid [d]

[a] Department of Computer and Systems Engineering, Ain Shams University, Cairo, Egypt
[b] STMicroelectronics, Cairo, Egypt
[c] Department of Electrical and Computer Engineering, University of Victoria, Victoria, BC, Canada
[d] Faculty of Information Engineering and Technology, German University in Cairo, Cairo, Egypt

ARTICLE INFO

Keywords:
Compressed Sensing (CS)
Measurement matrix
Mutual coherence
Restricted isometry property

ABSTRACT

Compressed Sensing (CS) is a novel data acquisition theorem exploiting the signals sparsity differing from traditional Nyquist theorem in the ability of obtaining all information of such signal in fewer samples. CS can enable full use of sparsity, where the sparse signal can be reconstructed using fewer measurements. Over the past decade, several papers have investigated the feasibility of deploying CS in current applications. A lot of developments are performed in this area in order to enhance the performance and re-usability. The CS algorithm involves many phases at the transmitter side, including: transformation, compression, encoding, encryption, and modulation. Meanwhile the receiver involves: demodulation, decryption, decoding, and reconstruction. This work assembles most of the published papers in the CS area, listing the important details and showing their contributions. Each building block of the CS system is studied solely and compared with its reference in the literature. A comparative study is performed reviewing the work in the literature with respect to compression metrics, deployed reconstruction algorithm, system complexity. Tabulated results are studied with respect to hardware and memory computation complexity. Recommendations and conclusions are illustrated at the end of our work.

1. Introduction

Most of the current information is based on Shannon and Nyquist theories [1], which state that in order to reconstruct a band limited signal without distortion, the sampling frequency must be strictly greater than twice the maximum frequency of the signal to avoid aliasing. Signals are then compressed by removing the inherent redundancies, then transmitted over the channel. Although this scheme is very effective, its main drawback is the high processing overhead required from sampling and compression which makes it not suitable for current applications due to the limited computation capabilities.

Compressed Sensing (CS) is a new framework proposed in [2] on the basis of signal decomposition and approximation theory. CS is considered as an alternative to the Nyquist criteria by offering small sensing time and sampling rate. In CS, signals are sampled at rates below Nyquist rate with the aid of linear projection onto a random basis. Meanwhile, the new scheme guarantees exact reconstruction of the original signal. CS helped in reducing power consumption and computation complexity of digital data. Information extraction is performed with the aid of a sensing matrix.

The following conditions need to be satisfied for exact reconstruction in CS: First, high sparsity of the sampled signal, where the number of non-zero elements is very small compared to the total number of elements. Sparsity can be viewed as the number of elements that hold the relevant information of the signal. Second, the incoherence of elements in the sampled signal which represents the duality between time and frequency domains. Incoherence represents the correlation between matrix elements.

The building blocks of the CS transmitter includes five building blocks. Sparse transformation enables to converting any signal to a sparse form in a certain domain through multiplication with a transformation matrix. Signal compression is performed on the sparse signal to compress the signal in a smaller size using the measurement matrix. The encoding step is optionally involved to improve the compression performance. Signal encryption is also an extra optional step that is deployed for both security and performance aspect. Eventually, the signal is modulated using conventional communication schemes. At the receiver side, after the demodulation step, signal reconstruction takes place after decoding and decryption.

The advantages of CS over the conventional sample and compression methodology are twofold: First, the complexity reduction in the compression phase at the transmitter node and deferring the load in the reconstruction phase at the receiver node. This model is beneficial in systems involving massive number of sensors, such as Wireless Sensor Networks (WSNs). Second, the compressed data size is dependent on

* Corresponding author at: Department of Computer and Systems Engineering, Ain Shams University, Cairo, Egypt.
E-mail address: watheq.elkharashi@eng.asu.edu.eg (M.W. El-Kharashi).

https://doi.org/10.1016/j.memori.2023.100060
Received 29 November 2022; Received in revised form 28 April 2023; Accepted 13 May 2023

both representation basis and signal sparsity. In conventional compression methods, compression is performed regardless of the sparsity level, which is ineffective.

Due to the benefits offered by CS, it has been deployed extensively in lot of applications recently. Considering Magnetic Resonance Imaging (MRI), CS is used to enhance the acquisition speed of the MRI. A new reconstruction algorithm for CS-MRI is proposed in [3] to enhance the signal recovery performance. The work in [4] considered the 2D-standard MRI, where simulation results showed the performance enhancement for the proposed technique. CS is also used in digital modulation as it improves the modulation scheme Bit Error Rate (BER) performance. The authors in [5] implemented the Quadrature Amplitude Modulation (QAM) scheme using CS to lower the power consumption and enhance the BER performance. In [6], it is demonstrated that CS is very effective in recovering signals sent over communication channels while saving about 90% of the work calculations. The authors in [7] studied the use of CS with impulsive Frequency Shift Keying (FSK) receiver to avoid the cost of frequency selective filters and challenges to obtain the channel state information. Another technique embedding CS in detection of Quadrature Phase Shift Keying (QPSK) modulated Orthogonal Frequency Division Multiplexing (OFDM) to achieve lower BER is proposed in [8]. Since Transient Electromagnetic (TEM) array detection systems face challenges due to large amount of data in the downhole, CS is deployed in [9] to overcome these challenges by reducing the data volume leading to improvement in the transmission efficiency.

In the field of Augmented Reality (AR) Drones, CS is used in reducing the amount of data transmitted between the drone and the command unit. The results in [10] showed a performance improvement done in the communication scheme when transmitting 2D signals from the drone using WLAN 802.11a. Similarly, CS can be deployed in a WSN to reduce the interaction latency between the sensors and the edge node in order to reduce the energy consumption. In [11], the use of CS in WSN is investigated leading to power consumption reduction. The authors in [12] used CS in a hybrid way by classifying sensor nodes into clusters to reduce the traffic overhead.

Wireless Body Area Network (WBAN) consists of smart sensors attached or implanted in the body that gather medical data such as: heart rate, Electroencephalography (EEG), oxygen level, and Electrocardiographic (ECG) for continuous monitoring. The deployment of CS in [13,14] reduced the sampling rate and power consumption. CS is also used in hyperspectral image instruments, which measure bunch of spectral bands for the purpose of earth exploration. CS is used in the implementation of low power Graphic Processing Units (GPUs) in [15] as an alternative for traditional compression methods.

In radar applications, CS is used to reduce the data acquisition through random collection instead of continuous sampling. The concept is investigated in [16,17]. The deployment of CS in Synthetic Aperture Radar (SAR) imaging to overcome the long calculation time and insufficient scalability of calculation ability is performed in [18–21]. CS also improved the performance and added noise resilience to radar speech acquisition based on the millimeter wave radar [22]. The authors in [23] associated CS with deep learning for Tomographic Synthetic Aperture Radar (TomoSAR) imaging for better performance results. Another application that uses CS is the Synthetic Aperture Sonar (SAS), which helped in breaking through low mapping issues such as size of sonar carrier and its speed [24]. CS also aided in improving the performance of the classification and recognition of several common signals in underwater target detection [25].

Over the past two decades, a lot of development has been performed in the CS area in the literature. This led to an increase in the variety of the deployed algorithms either in the compression scheme or the reconstruction criteria. The main contributions of this work are twofold.

1. Providing detailed information about the functionality of each building block in the CS system and studying the contribution of related work in this domain.
2. Assembling the developed work in CS area, categorizing them and applying a fair comparison with respect to memory cost, hardware implementation, and system robustness in order to make it easy for the new contributors to extract the required data.

This paper is organized as follows. Section 2 gives a brief about the existing CS categories. Section 3 illustrates all the building blocks of a CS system. A comparison between the CS techniques in the literature is presented in Section 4, followed by a list of the papers physically implementing the CS system in Section 5. Finally, Section 6 shows the paper conclusion and future work.

2. Compressed Sensing techniques

Over the past two decades, several types of CS techniques are being proposed. Three main categories of CS are proposed, as illustrated in Fig. 1. Conventional CS considers the matrix elements are represented in multi-bits where no slicing is performed on the signal. Block CS (BCS) is a special kind of conventional CS which is efficient when dealing with 2D signals. However, 1-bit CS is a special case, where only single bit is used to represent the original information to reduce the memory storage.

2.1. Block Compressed Sensing

When dealing with 2D images, conventional CS techniques suffer from the following challenges: the computational complexity of reconstruction is very high and the required storage space is very big for the random measurement matrix. In order to overcome the aforementioned challenges, BCS was first introduced in [26]. The proposition of BCS was motivated by the great success of block Discrete Cosine Transform (DCT) coding deployed in JPEG and MPEG standards. The main idea is slicing the whole 2D image into small blocks. As illustrated in Fig. 2, the original $n \times n$ image is partitioned into four blocks each of size $B \times B$, where B is the block size. The 2D sliced image shall be unrolled into 1D array, where the new 1D matrix size is $B^2 \times 1$.

The proposed technique has three main advantages over the ordinary CS. First, measurement operator can be easily stored and implemented through a random under-sampled filter bank. Second, since each block is processed independently, the initial solution can be easily obtained, and the reconstruction process can be substantially speeded up. Third, block-based measurement is more suitable for real time applications as the encoder does not need to send the sampled data until the whole signal is measured.

2.2. 1-bit Compressed Sensing

The conventional CS assumes that the measurements are real valued and have infinite bit precision. However, in practice conventional CS is considered as quantized CS, where the measurements are quantized into finite number of bits. 1-bit CS proposed in [27], is the extreme case of quantized CS, where the deployed quantizer represents the measurement information in a single bit using its sign only (± 1).

In conventional CS, the number of measurements is significantly less than the number of elements in original signal, which results in distortion in the reconstruction. In 1-bit CS, as the size of each element is 1-bit, the number of measurements is permitted to exceed the number of elements in the original signal, which reduces the distortion appearing in conventional CS. From the hardware perspective, 1-bit CS is the best way to implement the CS system. High speed comparators can be used due to its simplicity and low-cost [28,29].

The main drawback of the proposed approach is the loss of the magnitude information after quantization since the preserved information is only in the sign. However the authors in [27] managed to prove that signal recovery is possible using the concept of consistent construction. They proved that constraining the reconstruction to be

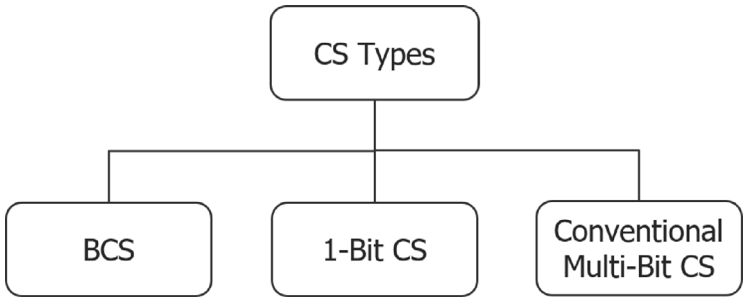

Fig. 1. CS types.

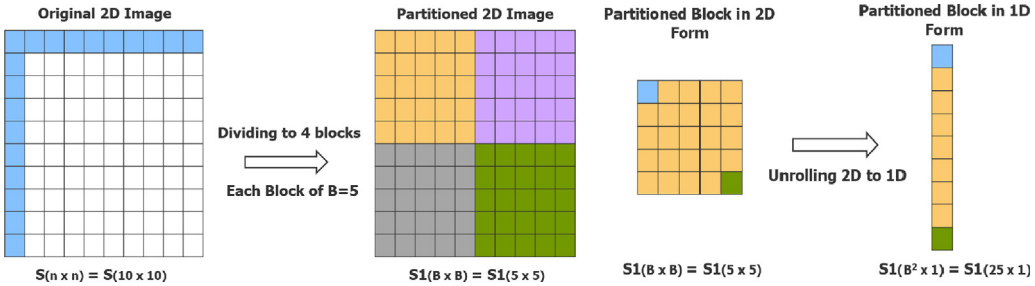

Fig. 2. BCS image division and unrolling.

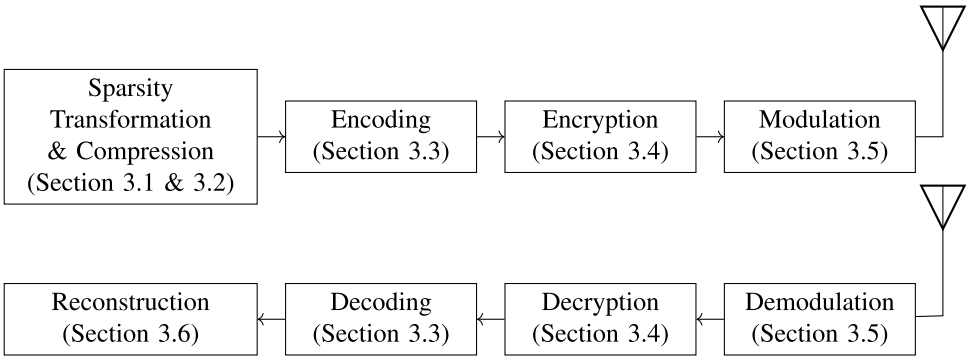

Fig. 3. CS overall system block diagram.

on the unit sphere resolves this ambiguity and significantly reduces the reconstruction search space. The work in [30] deployed the 1-bit CS in SAR imaging using weighted L1-Norm Minimization based on approximated observation. The algorithm proved its capability of reconstructing high-quality signals in small time while utilizing small memory.

3. Compressed Sensing system blocks

In order to compress and decompress real time signals, many operations are deployed, as illustrated in Fig. 3.

3.1. Signal sparsity transformation

Signal information is described in their coefficients. Sparsity of a signal means that most of the energy and information of the signal are concentrated in certain area, where large coefficients hold them. Meanwhile, other coefficients are nulls or close to zero. This implies that the signal can be represented with small number of bits. However, natural signals are not sparse in the time domain. In order to represent the signal in sparse form, it needs to be transformed to another domain.

Considering a 1D real signal s in time domain of size $N \times 1$ to be compressed, the signal is transformed to another domain by multiplying with the orthogonal basis transformation square matrix ψ of size $N \times N$ to produce sparse signal x of same size of s. The used formula is defined as follows:

$$s_{(N\times 1)}\, \psi_{(N\times N)} = x_{(N\times 1)} \tag{1}$$

where N is the length of the signal in both time and the transformed domains. The sparsified signal x has only K non-zero elements, where $k \ll N$. Fig. 4 shows the transformation process, where the cells colored in white are nulls. In the illustrated example, $N = 10$ and $K = 2$ satisfying the condition mentioned earlier. The transformation in case of BCS is performed by slicing the transformation matrix ψ into equal sub-matrices ψ_B of size $B^2 \times B^2$, where the generated partitioned matrix is sparse.

Since the Haar Wavelet Transform (HWT) is characterized by low memory storage requirement. Fast Haar Transform (FHT) is one of the algorithms which can reduce the tedious work of calculations. The authors in [31] modified the design of Fast Haar Wavelet Transform (FHWT) in order to achieve low power consumption and computation complexity compared to the conventional method to suit in bio-medical applications. This is performed by not computing the decimated wavelet coefficients.

In [32], a comparison is performed between DCT and Discrete Wavelet Transform (DWT) showing that the performance of the DWT

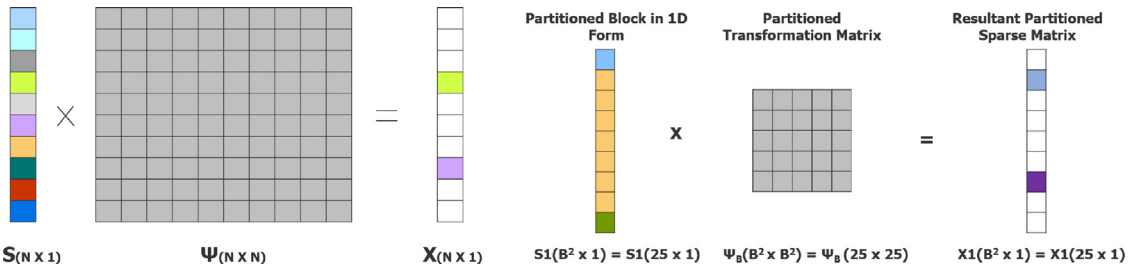

Fig. 4. BCS sparse signal transformation.

is better than the DCT. However, the time complexity of the DCT is smaller than the DWT.

The Modified Fast Haar Wavelet Transform (MFHWT) proposed in [33–35] is one of the algorithms, which can reduce the calculation work in Haar Transform (HT). The results show that MFHWT provides sparse representation; MWHT is faster than HT and reduce computational work; MSE and PSNR of reconstructed values are good as in case of HT; and the required memory storage in MFHWT is nearly half the original used data in FHT.

The Contourlet Transform (CT) is generated by multi-scale geometric analysis that showed high performance in nonlinear approximation of 2D signals due to its non-redundancy. Wavelet Based Contourlet Transform (WBCT) which is a non-redundant version of CT is proposed in [36]. With the aid of BCS and Iterative Thresholding recovery algorithm, the authors showed that the PSNR and the reconstruction time of WBCT is better than both CT and 2D Discrete Wavelet Transform (2D-DWT).

In [37], the authors investigated the performance of both Daubechies wavelets and Haar wavelets. Simulation results show that the performance of Daubechies is better than the Haar. However, the later has time complexity less than that the Daubechies.

BCS is associated with the Haar Discrete Wavelet Transform (HDWT) and Energy based Re-weighted Sampling (ERWS) in [38] to extract high energy components from 2D signals. Using the Orthogonal Matching Pursuit (OMP) in signal reconstruction, the paper compared the HDWT with DCT with respect to three metrics. (1) PSNR: HWT and DCT based ERWS has achieved almost closer PSNR values. (2) Time complexity: HWT based RWS/ERWS has less execution time and energy consumption than DCT based RWS/ERWS. (3) CPU cycles: HWT based RWS/ERWS has very less CPU cycles than DCT based RWS/ERWS.

In [39], a different approach is considered, where the transformation matrix is replaced by a permutation matrix to construct the BCS signal. Results show that the proposed approach increases the PSNR and the signal quality while reconstruction.

The authors in [40] investigated the performance of the following transformation basis matrices: Discrete Fourier Transform (DFT), Discrete Walsh Hadamard Transform (DWHT), Discrete Hartley Transform (DHT), DCT, and DWT with Chebyshev chaotic measurement matrix ϕ. BCS is being deployed in order to deal with 2D signals. With the aid of OMP algorithm in signal recovery, simulation results show that DWT is able to obtain the best quality of the reconstructed signals in terms of PSNR. The DCT proved its capability of good recovery when increasing the number of BCS sub-blocks.

The Discrete Fractional Fourier Transform (DFRFT) proposed in [41] is used to construct the transformation matrix ψ to generate the sparse signal. The authors targeted the reconstruction of Wide-band Linear Frequency Modulation (WB-LFM) signals and used the advantage of good aggregation characteristics in the FRFT domain. They used Gaussian random measurement matrix associated with OMP in the reconstruction. Simulation results proved that the proposed approach is able to reconstruct the signal efficiently.

3.2. Signal compression

After the signal is sparsified in certain domain, compression is performed by multiplying the resultant signal x with measurement matrix ϕ of size $M \times N$ in order to generate the resultant compressed signal y of size $M \times 1$. The formula is defined as follows:

$$\phi_{(M\times N)}\, x_{(N\times 1)} = y_{(M\times 1)} \tag{2}$$

where M is the number of measurements representing the size of elements in the resultant signal y that shall be used to reconstruct the original signal x again. Due to compression, the size of y is less than x, where $K < M < N$. Signal compression is illustrated in Fig. 5, where the example shows that $K = 2, M = 6, N = 10$, satisfying the aforementioned condition.

In case of BCS, the measurement matrix is divided with the same ratio as the original 2D signal, then multiplied with the partitioned 1D matrix to generate the compressed signal y. As shown in Fig. 5, the measurement matrix ϕ is divided into 4 sub-matrices ϕ_B of size $M_b \times B^2$, where M_b refers to the number of divided blocks. The divided block measurement matrices ϕ_B are arranged in block diagonal matrix to form the full measurement matrix ϕ as follows:

$$\phi = \begin{pmatrix} \phi_B & & & \\ & \phi_B & & \\ & & \ddots & \\ & & & \phi_B \end{pmatrix} \tag{3}$$

The figure shows that the generated compressed partitioned signal y preserves the same partitioned size of $M_b \times 1$ if multiplied with the partitioned measurement matrix ϕ_B.

The main difference in case of 1-bit CS is the presence of additional 1-bit quantizer after the generation of the compressed signal y. The aggressive quantizer is modeled using sign function, which returns ± 1. The resultant compressed signal holds only the amplitude sign information. The system is formulated as follows:

$$y_{(M\times 1)} = sign[\phi_{(M\times N)}\, x_{(N\times 1)}] \tag{4}$$

Fig. 6 lists the types of proposed measurement matrices in the literature. Two main categories are introduced: deterministic and random matrices. The former matrices are generated with certain constraints in which when multiplied with the sparse signal they generate a compressed signal satisfying the requirements of the reconstruction algorithms. The later contains lot of variations, as shown in the figure.

Random dense matrices are the most commonly used type of matrices including random Gaussian and random Bernoulli matrices, as they are universally incoherent with any sparse signal thus, the number of compressed measurements required for exact reconstruction is almost minimal. Despite their advantages, they suffer from the need for huge memory buffering for storage of matrix elements and high computational complexity due to their completely unstructured nature.

Due to the limitations of dense matrices, Structurally Random Matrices (SRM) are proposed recently as they have different structure, enabling easy implementation and reasonable memory storage.

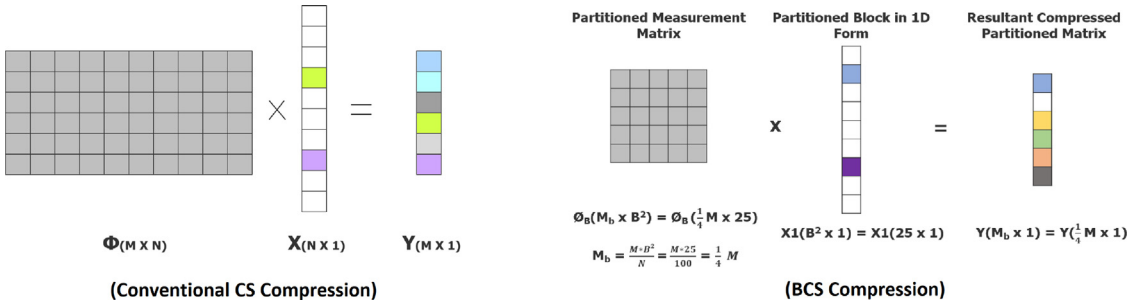

Fig. 5. Signal compression using measurement matrix in conventional CS and BCS compressions.

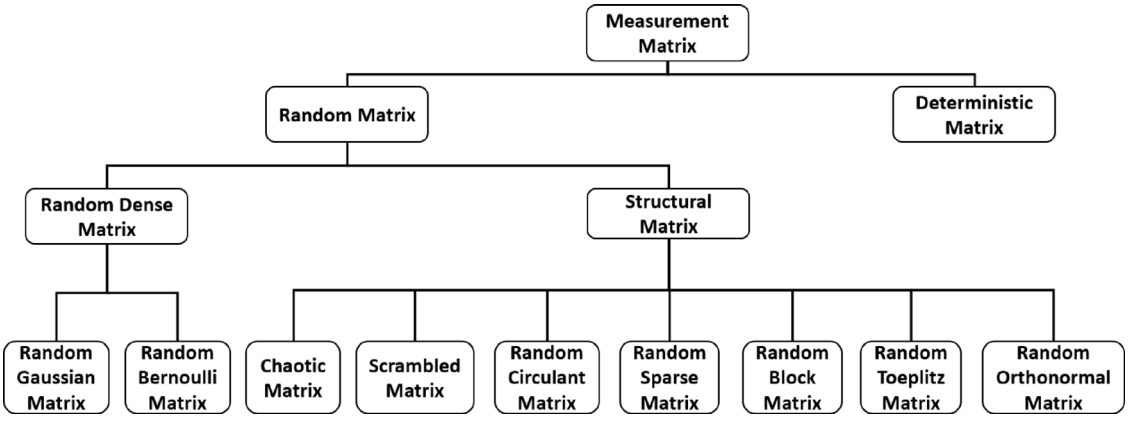

Fig. 6. Measurement matrix types.

Toeplitz matrix is one of the structured matrices, which has the following structure:

$$A = \begin{pmatrix} a_0 & a_1 & \dots & a_{2-n} & a_{1-n} \\ a_1 & a_0 & \dots & a_{3-n} & a_{2-n} \\ \vdots & \vdots & \ddots & \ddots & \vdots \\ a_{n-1} & a_{n-2} & \dots & \dots & a_0 \end{pmatrix} \tag{5}$$

The matrix structure has three benefits. First, user only needs to have the first row and first column then every other element is repeated diagonally. So, it requires the generation of only $O(N+M-1)$ independent random variables. Second, multiplication with Toeplitz matrices can be efficiently implemented using Fast Fourier Transform (FFT), resulting in faster acquisition and reconstruction algorithms. Third, Toeplitz-structured matrices arise naturally in certain application areas such as system identification.

Circulant matrix is a special case of Toeplitz matrix, where each row is a cyclic shift of the previous row. The matrix has the following form:

$$A = \begin{pmatrix} a_0 & a_{n-1} & \dots & a_2 & a_1 \\ a_1 & a_0 & \dots & a_3 & a_2 \\ \vdots & \vdots & \ddots & \ddots & \vdots \\ a_{n-1} & a_{n-1} & \dots & \dots & a_0 \end{pmatrix} \tag{6}$$

The matrix has the two advantages. The first one is efficient hardware implementation, where each row is a cyclically shifted vector of the seed vector. The measurements can be produced by convoluting the input signal with the seed vector. The second one is low memory storage complexity $O(N)$.

Considering the block diagonal matrices, which are structural matrices generated by concatenating sub-matrices, such as the following form:

$$A = \begin{pmatrix} A_1 & 0 & \dots & 0 \\ 0 & A_2 & \dots & 0 \\ \vdots & \vdots & \ddots & \vdots \\ 0 & 0 & \dots & A_n \end{pmatrix} \tag{7}$$

The matrix structure offers the following benefits: easy hardware implementation, fast computation, small memory, and the number of measurements required for exact reconstruction is nearly optimal.

Another type of matrices is the scrambled matrix, which is generated by multiplying the original measurement matrix by a scrambler in order to shuffle the elements randomly to achieve better incoherence. An extra step maybe added by changing the signs of some elements. This process offers the following advantages: recovery rate is almost equal to the random Gaussian matrix and computation complexity is better than the random matrices with relatively small memory storage. Similarly, the chaotic matrices which are constructed by multiplying the random matrix with chaotic sequence to achieve the same benefits.

There are many types of orthonormal matrices, such as: DFT, DCT, and Hadamard matrices. These matrices have three main advantages. The first one is the significant reduction in the complexity of a sampling system as it exploits the fast computational property of FFT. The second one is satisfying Restricted Isometry Property (RIP) under certain conditions. The third one is including operators that are nearly optimal for acquisition of sparse signals in the time domain in case of general partial unitary matrices.

However, these suffer from four major drawbacks. First, they cannot be used directly to sample the spectrally sparse signals. Second, they fail to reconstruct sparse signals in the FFT or DCT domain. Third, their orthogonality is unstable due to randomness of construction. Fourth, partial Fourier matrix is only incoherent with signals which are sparse in the time domain, severely narrowing its scope of applications.

Sparse random matrices are matrices whose most elements are zeros. The matrix is characterized by being hardware friendly due to small memory storage and fast computation in reconstruction tending to near optimal performance.

3.3. Signal encoding/decoding

From the perspective of information theory, CS is not an efficient system for data compression compared to standard compression techniques. Because the process is not considered as real compression other

than dimensionality reduction. In order to overcome this and improve the compression performance, the compressed signal is encoded before transmission over the RF section. The most straight forward solution is to simply associate a uniform Scalar Quantizer (SQ) with the CS system. However, this solution results in performance degradation due to the ignorance of the compressed signal. Another alternate solution would be combining the CS system with both uniform SQ and entropy encoder to generate compressed bitstream to improve the performance.

The Differential Pulse Code Modulation (DPCM) proposed in [42] is associated with uniform scalar quantizer for signal encoding. The authors mentioned that the proposed framework is compatible only with BCS. The measurement matrix used is Gaussian random matrix and the Multihypothesis BCS Smoothing Projected Landweber (MH-BCS-SPL) is used in the reconstruction. Same procedures applied at the encoder side shall be applied at the decoder. Simulation results show that the addition of the encoder increased the PSNR compared to the ordinary CS system. Although the proposed encoder achieves good results, natural signals which have various directions of spatial pixel correlation show that the DPCM with a fixed prediction direction may not be the best for measurement coding.

The authors in [43] proposed a better CS encoding algorithm better than the DPCM entitled Spatially Directional Predictive Coding (SDPC). The Gaussian random matrix is used, associated with the BCS-SPL reconstruction algorithm. Simulation results show the performance improvement compared to the DPCM and no encoder cases. The same encoder is used at the receiver side for signal decoding.

In [44], the Measurement Prediction (MP) encoder is proposed to overcome the challenges in the DPCM encoder. Structural measurement matrix is integrated with BCS along with BCS-SPL to test the efficiency of the encoder. Results show that the MP encoder is able to save the bitrate for small block sizes while preserving the signal quality at large block sizes.

The authors in [45] investigated the deployment of Golomb–Rice encoder inside the CS system due to its simplicity, efficiency, and ability to encode the signal with bitrate close to the first order entropy of the signal. The author implemented the encoder on hardware showing that the division operation in the algorithm is implemented with simple counter and shift register. Simulation results compare the performance before and after the integration of the encoder showing the performance enhancement.

3.4. Signal encryption/decryption

Several papers in the literature studied the security aspect of the CS system. This includes the robustness of the CS system and ability to avoid side channel attacks and hardware Trojans. Digital watermarking algorithm based on interleaving extraction of BCS in the Contourlet domain is proposed in [46]. simulation results illustrate the performance enhancement of reconstruction mechanism as well as the robustness against JPEG compression and noising.

BCS is associated with Multiple Description Coding (MDC) as the protection scheme and inherent characteristics of the original signal in [47] to enhance the performance of reliable transmission of BCS. Several trials are deployed by changing the BCS block size with MDC on the transmitted signal over a lossy channel, where reconstruction is performed using the ℓ_1-norm constraint. The authors extended their work in [48] applying BCS on square blocks with different sizes based on quadtree decomposition for the classification of signal characteristics without taking inherent characteristics into account. MDC is also deployed for signal protection associated with the Least Absolute Shrinkage and Selection Operator (LASSO) as the reconstruction mechanism. Results show that associating the protection mechanism aids in enhancing the performance of reconstructed signal.

The normalization of the measurement matrix is proposed in [49] to achieve better signal protection. However, the mechanism suffers from extra limitation due to the need to transfer the measurement information on an extra secure channel to the receiver side. This limitation is solved in [50], where an approximately Gaussian distributed sensing measurement matrix is constructed using the combination of Linear Feedback Shift Register (LFSR) and Non-linear Feedback Shift Register (NFSR). The authors proved that side channel attacks to retrieve the key from the generated matrix is more difficult than brute force attacks. An extension for the aforementioned work is performed in [51] in order to avoid energy leakage and resist Chosen Plaintext Attacks (CPA). The signal is compressed and normalized as proposed earlier then diffusion is performed according to the statistical characteristics of the measurements to resist CPAs and hide both energy information and quantization parameters. DCT is used as the transformation matrix associated with the random Gaussian measurement matrix. OMP is used as reconstruction algorithm at the receiver.

3.5. Signal modulation/demodulation

Most of the literature in this area are directed towards using CS in channel estimation of OFDM/MIMO systems. Papers use reconstruction algorithms such as: CS Matching Pursuit (CoSAMP), Total Variation (TV), and Orthogonal Matching Pursuit (OMP) to achieve better estimation results.

The authors in [52] investigated the use of OFDM in building up the CS system. BCS is used for compressing signals that are transmitted over Additive White Gaussian Noise (AWGN) channel using OFDM to improve signal recovery performance. DPCM is used in the encoding process using 8 bits. A comparison between both reconstruction algorithms: SPL and OMP is performed with respect to BCS block size and sampling rate. Simulation results show that BCS-SPL outperforms BCS-OMP in most of the cases.

3.6. Signal reconstruction

The universality property postulates that the measurement matrix ϕ can be paired with any representation of the input sparse basis matrix ψ. This implies that the reconstruction quality is equally good for all basis.

Due to the dimensionality reduction from sparse signal x of length N to the compressed signal y of length M, reconstruction is theoretically impossible. However, the authors in [53] analyzed the geometry of measurement matrix ϕ in order to reach excellent signal recovery using the minimum number of measurements M. They proposed a well-defined criterion named RIP that guarantees stable recovery in the presence of additive noise.

Since linear isometry states that two vectors must preserve the same distance after transformation. Consequently, the RIP states that the transformation performed by matrix ϕ preserves the Euclidean norm of sparse signals. The condition in [54] postulates that, for any K-sparse signal x, if there is a constant $\delta \in (0, 1)$ that satisfies the reconstruction of x from y, then the measurement matrix is said to satisfy the RIP with order K. The minimum non negative number δ is called the Restricted Isometry Constant (RIC) of order K. The RIP is formulated as follows:

$$(1 - \delta_k)\|x\|_2^2 \leq \|\phi x\|_2^2 \leq (1 + \delta_k)\|x\|_2^2 \tag{8}$$

where $\delta_k \in (0, 1)$. Based on the aforementioned equation, RIP implies that for all $N \times K$, the sub-matrices of ϕ are close to an isometry, and therefore distance-preserving. Also, the eigenvalues of their Gram matrices lie in this interval $[(1 - \delta), (1 + \delta)]$. This means that the bigger value of K, the better guarantee that the measurement matrix ϕ satisfies the RIP, which in terms guarantees better reconstruction.

The matrix ϕ with mutual coherence μ is said to be satisfying the RIP of order K when the following conditions take place:

$$\delta_k \leq \mu(k - 1), \quad k < 1 + \frac{1}{\mu} \tag{9}$$

Based on the Welch bound formula [55] defining the lower bound for the mutual coherence of matrix ϕ, deterministic construction based on coherence can generate RIP of order K defined by the following inequality:

$$k \leq O(\sqrt{M}) \tag{10}$$

Using the mutual coherence, any matrix can be proved to be able to get perfect recovery of signal x when the above condition satisfies.

The authors in [56] proved that binary sparse matrices are not able to satisfy the RIP with parameters k and δ, unless the number of rows is $O(k^2)$. The work is extended in [57], showing that such matrices satisfy another modified of RIP that is called RIP-p where the Euclidean ℓ_2-norm is replaced by the ℓ_p-norm. The authors proposed a generalized RIP-p formula as follows:

$$\|\phi\ x\|_p = (1 \pm \delta)\|x\|_p, \quad 1 \leq p \leq 1 + \frac{O(1)}{\log(n)} \tag{11}$$

where RIP-1 and RIP-2 are a special cases of this formula. The proof of RIP-1 is reproduced in [58].

Since it is difficult to test if a given matrix satisfies RIP, an alternative statistical version of RIP is proposed for deterministic sensing matrices. When a deterministic sensing matrix satisfies Statistical RIP (StRIP), it means that (8) holds with respect to a uniform distribution of the vectors x among all K-sparse vectors in R^N of the same norm. The authors in [59,60] formulated the StRIP using the following inequality using the Johnson–Lindenstrauss (JL) lemma:

$$Pr(\|\phi x\|_2^2 - \|x\|_2^2 \leq \delta\ \|x\|_2^2) \geq (1 - \epsilon) \tag{12}$$

The extended work performed in [61] shows that both the matrices constructed from Reed–Muller codes introduced in [62] and Chirp based matrices proposed in [63] satisfy the StRIP. The authors in [64] constructed a measurement matrix based on chaotic sequences satisfying the StRIP. Also, the Toeplitz matrix proposed in [65] is based on StRIP.

Despite the easiness of satisfying the StRIP, it suffers from two main drawbacks. First, unlike simple RIP case, StRIP does not automatically imply unique reconstruction, not even with high probability. Second, StRIP is weaker than the RIP and guarantees recovery of all but an exponentially small fraction of sparse signals.

Since checking the RIP requires complex operations, an alternative easy solution is checking the statistical correlation between row vectors and column vectors of the measurement matrix, known as the incoherence (mutual coherence). Not only the coherence of the measurement matrix must be low for better reconstruction, but also the coherence of the resultant matrix from multiplying the measurement matrix with the sparse input vector must be low as well. As shown in [66], Toeplitz and circulant matrices are not satisfying the mentioned condition.

The coherence operator μ mentioned earlier is considered as a quantitative index of the ability of the sensing matrix for recovery. Since high coherence means that there is a repeated column/row in the matrix, the information obtained from these rows/columns after sampling would also be similar. This makes the reconstruction process very difficult. This is the reason behind why random matrices have low coherence coefficient. Therefore, the smaller the mutual coherence, the better quality of reconstruction is achieved.

The transmitted compressed signal y is of size $M \times 1$, where $M \ll N$. The main target is to reconstruct the signal x of size $N \times 1$ using the following inputs: the compressed signal y of size $M \times 1$, the measurement matrix ϕ of size $M \times N$, and the maximum sparsity K in the original signal x. Recalling the compression technique, the generation of matrix y can be modeled by the following equation:

$$\phi_{(M\times N)} \times x_{(N\times 1)} = y_{(M\times 1)} \tag{13}$$

Since ϕ is a full rank matrix and $M \ll N$, this implies that the number of equations is larger than the number of unknowns, which leads to an infinite number of solutions to recover y from x. Reconstruction of the original signal shall be modeled as follows:

$$\min_{x}\ J(\underline{x})\ \ s.t.\ \ \phi\underline{x} = \underline{y} \tag{14}$$

where $J(x)$ is an optimization function required to solve the reconstruction problem to recover the matrix x from y. Minimizing $J(x)$ is performed to find the cheapest solution over all of them. Solving $J(x)$ involves finding the ℓ_0-norm, ℓ_1-norm, or ℓ_2-norm, so that the problem shall be formulated as follows:

$$\min_{x}\ \|x\|_0\ \ s.t.\ \ \phi\underline{x} = \underline{y} \tag{15}$$

There are three types of signal reconstruction algorithms in CS: the conventional multi-bit CS reconstruction algorithms, the BCS reconstruction algorithms, and the 1-bit CS reconstruction algorithms. The later is studied in [67–69]

Algorithm 1: Orthogonal Matching Pursuit (OMP)

Input: measurement matrix ϕ, compressed signal y, and maximum sparsity K

Output: original sparse signal x

Initialize: residual vector $r_0 = y$, iteration index $j = 0$, and support $S = \{\}$

while $||r_j||_2 > \epsilon$ *or* $j < K$ **do**

1) Increment j
2) Calculate $E_j = min\ ||c\ \phi_j - r_{j-1}||_2^2$ using $max\ |\phi_j^T r_{j-1}|$ for $1 \leq j \leq N$
3) Obtain the position i of the maximum element
4) Include i in the support $S_j = S_{j-1} \cup \{i\}$
5) Reconstruct ϕ columns as follows: $\phi_j = [\phi_{j-1}\ \phi_i]$
6) Calculate $\hat{x}_j = min\ ||y - \phi_{S_j} x_j||_2^2$ simplified as $\hat{x}_j = \phi_{S_j}^{\dagger} y$
7) Update the residual: $r_j = y - \phi_{S_j}\hat{x}_j$

end

3.6.1. Conventional CS reconstruction algorithms

In order to solve (15) several algorithms have been proposed over the years. Fig. 7 illustrates the two main families of proposed algorithms:

3.6.1.1. Greedy algorithms. These algorithms emphasis the discrete nature of the problem and iterates over the equations to build the support containing the indices of required sparsest solution. The OMP algorithm proposed in [70] is the most commonly used algorithm in signal reconstruction in CS. Algorithm 1 starts by the following formula:

$$\phi_{(M\times N)}\ x_{(N\times 1)}\ +\ y_{(M\times 1)}\ =\ r_{(M\times 1)} \tag{16}$$

where r represents the residual, which shall contain the error values from computing x. The initial value of the residual shall be null and it shall increase as the loop proceeds.

The algorithm starts by sweeping over all columns in ϕ trying to find the index of the column when multiplied with the corresponding residual element will get the maximum value and minimum error. The index of the chosen column i is added to the support set to be used in re-arranging the columns of ϕ to obtain the maximum desired value mentioned earlier. The value of the estimated element $\hat{x}$ shall be calculated using the least square method, as shown in Step 6 which is simplified using the Moore–Penrose inverse of ϕ. The new residual value is calculated and checked if larger than the small number ϵ.

The calculated overall complexity of the OMP is $O(MNK)$, which is calculated based on the two stages. The sweep stage, which involves choosing a new column in ϕ and computing Step 1 in the algorithm. This operation requires $O(MN)$ operations and the least square stage, which requires computing Step 5, which involves $O(MK^2)$.

A relaxed version of the OMP is proposed in [71] simplifying its operations in a proposed algorithm entitled Stagewise Orthogonal

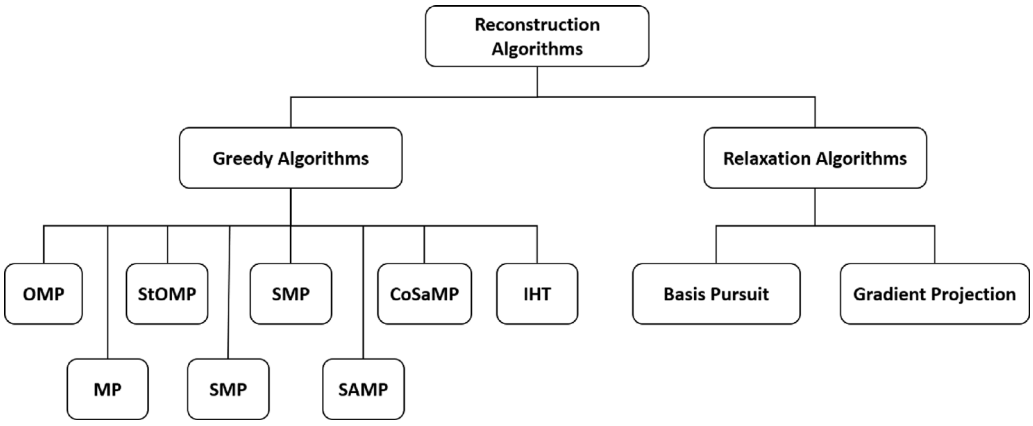

Fig. 7. Reconstruction algorithms types.

Algorithm 2: Stagewise Orthogonal Matching Pursuit (StOMP)

Input: measurement matrix ϕ, compressed signal y, and maximum sparsity K
Output: original sparse signal x
Initialize: residual vector $r_0 = y$, iteration index $j = 0$, and support $S = \{\}$
while $||r_j||_2 > \epsilon$ *or* $j < K$ **do**
1) Increment j
2) Obtain the position i for the elements $\phi_j^T r_{j-1}| > V_{th}$
3) Include i in the support $S_j = S_{j-1} \cup \{i\}$
4) Reconstruct ϕ columns as follows: $\phi_j = [\phi_{j-1}\ \phi_i]$
5) Calculate $\hat{x}_j = min\ ||y - \phi_{S_j} x_j||_2^2$ simplified as $\hat{x}_j = \phi_{S_j}^{\dagger} y$
6) Update the residual: $r_j = y - \phi_{S_j} \hat{x}_j$
end

Algorithm 3: Matching Pursuit (MP)

Input: measurement matrix ϕ, compressed signal y, and maximum sparsity K
Output: original sparse signal x
Initialize: residual vector $r_0 = y$, iteration index $j = 0$, and support $S = \{\}$
while $||r_j||_2 > \epsilon$ *or* $j < K$ **do**
1) Increment j
2) Solve $E_j = min\ ||c\ \phi_j - r_{j-1}||_2^2$ using $max\ |\phi_j^T r_{j-1}|$ for $1 \le j \le N$
3) Obtain the position i of the maximum element
4) Include i in the support $S_j = S_{j-1} \cup \{i\}$
5) Reconstruct ϕ columns as follows: $\phi_j = [\phi_{j-1}\ \phi_i]$
6) Calculate $\hat{x}_j = min\ ||y - \phi_{S_{j-1}} x_{j-1} + a_i z||_2^2$ simplified as $\hat{x}_j = x_j + a_i^T r_{j-1}$
7) Update the residual: $r_j = y - \phi_{S_j} \hat{x}_j$
end

Matching Pursuit (StOMP). Since the OMP extensively sweeps over all the elements in the matrix ϕ and calculates the inner product with the residual to reach out the index of the element with maximum inner product. As shown in Algorithm 2, this operation is simplified in the StOMP by setting a certain threshold for the inner product calculation, which leads to group of indices instead of single index added to the support S. The aforementioned relaxation simplifies the rest of operations in the loop. The complexity of the proposed algorithm is $O(MNK)$.

The Matching Pursuit (MP) algorithm is a much more relaxed version of OMP, where the main difference is in Step 4, as shown in Algorithm 3. The calculated old value of x is not used in OMP, meanwhile the MP gets advantage of this value to reduce the number of computations in Step 5, where the residual is used simplifying the complexity of the second step to be $O(MN)$. The modified step implies that the new element in x is calculated using the previous solution added to the newly added atom. This illustrates the difference between the MP and OMP, where the former may choose the same atom several times which leads to only changing the added coefficient.

The authors in [72] proposed the Subspace Matching Pursuit (SMP) algorithm simplifying the MP algorithm. Algorithm 4 states that: if RIP of order $2K$ is satisfied ($\delta_{2k} \ll 1$), the vector $\beta = \phi^T \phi x$ can serve as a proxy for the signal x because the energy of k-elements in x is the same as in y. The proxy signal will aid in the reconstruction process with the knowledge of the compressed signal $y = \phi x$. Similar to the OMP and MP, the algorithm uses the residual of the current samples to construct the proxy. The indices of the largest elements in the proxy are extracted and added to the support set to re-arrange the columns in of ϕ. The temporal estimate α is calculated using the simplified LS method in Step 6. The indices of largest elements in α are stored in new support set S' and others are pruned away. The new support set is used to re-arrange the columns of ϕ to aid in calculating the estimate signal $\hat{x}$. Eventually, the residual value is updated using the calculated indices. The process is repeated till finding the recoverable energy in the signal. The complexity of the proposed technique is $O(MNK)$.

The CoSaMP proposed in [73] is another simplified version of the SMP depending on satisfying RIP of order $2K$ ($\delta_{2k} \ll 1$). As shown in Algorithm 5, the difference is in Steps 7 and 8 where not only the indices of α are stored but also the value of the largest elements, which are used to update the estimate signal $\hat{x}$ directly. The difference is illustrated in [74]. The complexity of the proposed algorithm is $O(MN)$ similar to the MP. A comparison between the CoSaMP and the OMP is studied in [75], showing that the CoSaMP has similar performance to OMP and with low computation complexity.

Iterative Hard Thresholding (IHT) algorithm proposed in [76] simplifying the OMP procedure by replacing the first LS-problem in the OMP to be calculated outside the iterative loop. The algorithm calculates the matrix β in the very beginning and sorts all elements in descending order preserving their indices to be used later, as illustrated in Algorithm 6. Similar to the OMP the indices are added to the support to re-arrange the columns of ϕ matrix to be with the same order. Every element in the estimate signal $\hat{x}$ is eventually calculated by simplifying the LS problem to be a simple multiplication between the re-arranged ϕ with the compressed signal y. The residual usage in such case is only for condition checking only. The algorithm complexity is $O(MN)$.

Algorithm 4: Subspace Matching Pursuit (SMP)

Input: measurement matrix ϕ, compressed signal y, and maximum sparsity K
Output: original sparse signal x
Initialize: residual vector $r_0 = y$, iteration index $j = 0$, and support $S = \{\}$
while $||r_j||_2 > \epsilon$ *or* $j < K$ **do**
1) Increment j
2) Calculate the proxy using $\beta = max\ |\phi^T r_{j-1}|$
3) Obtain the position i of the maximum element
4) Include i in the support $S_j = S_{j-1} \cup \{i\}$
5) Reconstruct ϕ columns as follows: $\phi_j = [\phi_{j-1}\ \phi_i]$
6) Calculate temporal estimate using: $\alpha_j = \phi^{\dagger}_{S_j} y$
7) Save the indices of α in new support S'_j and prune the others
8) Compute the estimate signal: $\hat{x}_j = min\ ||y - \phi_{S'_j} x_j||_2^2$ simplified as $\hat{x}_j = \phi^{\dagger}_{S'_j} y$
9) Update the residual: $r_j = y - \phi_{S'_i} \hat{x}_j$
end

Algorithm 5: CS Matching Pursuit (CoSaMP)

Input: measurement matrix ϕ, compressed signal y, and maximum sparsity K
Output: original sparse signal x
Initialize: residual vector $r_0 = y$, iteration index $j = 0$, and support $S = \{\}$
while $||r_j||_2 > \epsilon$ *or* $j < K$ **do**
1) Increment j
2) Calculate the proxy using $\beta = max\ |\phi^T r_j|$
3) Obtain the position i of the maximum element
4) Include i in the support $S_j = S_{j-1} \cup \{i\}$
5) Reconstruct ϕ columns as follows: $\phi_j = [\phi_{j-1}\ \phi_i]$
6) Calculate temporal estimate using: $\alpha_j = \phi^{\dagger}_{S_j} y$
7) Save the largest entries in α and their indices in new support S'_j and prune the others
8) Save the largest entries in the estimate signal: $\hat{x}_j = \alpha_{S'_j}$
9) Update the residual: $r_j = y - \phi_{S'_i} \hat{x}_j$
end

Algorithm 6: Iterative Hard Thresholding (IHT)

Input: measurement matrix ϕ, compressed signal y, and maximum sparsity K
Output: original sparse signal x
Initialize: residual vector $r_0 = y$, iteration index $j = 0$, and support $S = \{\}$
1) Compute $\beta_{(N\times 1)} = \phi^T y$ and sort the array from largest to smallest $|\beta_{k_1}| > |\beta_{k_2}| > \cdots > |\beta_{k_n}|$
while $||r_j||_2 > \epsilon$ *or* $j < K$ **do**
2) Increment j
3) The position $i = k_1$ is largest element index in β
4) Include i in the support $S_j = S_{j-1} \cup \{i\}$
5) Reconstruct ϕ columns as follows: $\phi_j = [\phi_{j-1}\ \phi_i]$
6) Calculate $\hat{x}_j = min\ ||y - \phi_{S_j} x_j||_2^2$ simplified as $\hat{x}_j = \phi^T_{S_j} y$
7) Update the residual: $r_j = y - \phi_{S_j} \hat{x}_j$
end

The IHT, SMP, and the CoSAMP mentioned earlier are top-down approaches that use the backtrack strategy to identify the true support set accurately. On the other hand, the OMP and MP are considered as bottom-up approach as they propose a solution to the estimate the value of K by moving forward step by step. The proposed Sparsity Adaptive Matching Pursuit (SAMP) in [77] takes advantage of both approaches. As illustrated in Algorithm 7, the ℓ_2-norm of the current value of the residual obtained at Step 8 is compared with the old one, and the finalist set W is calculated, then fed back to the algorithm mixing up both approaches. The algorithm complexity is $O(MNK)$.

Algorithm 7: Sparsity Adaptive Matching Pursuit (SAMP)

Input: measurement matrix ϕ, compressed signal y, and maximum sparsity K
Output: original sparse signal x
Initialize: residual vector $r_0 = y$, iteration index $j = 0$, supports $S = \{\}, L = \{\}$, stage index $n = 0$, and step size $\upsilon = 1$
while $||r_j||_2 > \epsilon$ **do**
1) Increment j, n
2) Calculate $max\ (|\phi_j^T r_{j-1}|, W)$
3) Obtain the position i of the maximum element
4) Include i in the support $S_j = S_{j-1} \cup \{i\} \cup L_{j-1}$
5) Calculate $max\ (|\phi^{\dagger}_{S_j} y|, W)$
6) Obtain the position t of the maximum element
7) Include t in the support $L_j = L_{j-1} \cup \{t\}$
8) Compute the residual: $r_j = y - \phi_{L_j} \phi^{\dagger}_{L_j} y$
if $||r_j||_2 \geq ||r_{j-1}||_2$ **then**
9) $W = (n+1) * \upsilon$
end
else
9) Increment j
end
10) Update the residual: $\hat{x}_j = \phi^{\dagger}_{L_j} y$
end

3.6.1.2. Relaxation algorithms. Although the ℓ_0-optimization mentioned in (15) is able to find the sparsest final solution for signal x, usually it is very difficult to solve this problem as it is considered an NP-Hard. The ℓ_0-norm can be represented using the following function:

$$\|x\|_0 = \sum_{i=0}^{N} F(x_i), \quad F(x) = \begin{cases} 0 & x = 0 \\ 1 & x \neq 0 \end{cases} \tag{17}$$

The relaxation algorithms offer an alternative functions $R(x)$ for $F(x)$ used in relaxing the ℓ_0-expression. Various functions are commonly used such as:

$$R_1(x) = 1 - e^{\frac{-x^2}{\sigma}} \qquad R_2(x) = \frac{x^2}{x^2 + \sigma} \qquad R_3(x) = |x|^{\sigma} \tag{18}$$

where all the alternative functions share the following common property:

$$R_1(x) = R_2(x) = R_3(x) = \begin{cases} 0 & |x| \ll \sigma \\ 1 & |x| \gg \sigma \end{cases} \tag{19}$$

As illustrated in Fig. 8, the relaxation algorithms managed to approximate the ℓ_0-optimization problems through the shown iterative steps.

The algorithm starts by initializing the estimate value $\hat{x}$ using the measurement matrix ϕ and the compressed signal y. The algorithm uses the largest value of σ and solves the alternative relaxation function to generate the estimate $\hat{x}$. The computed solution is used as a warm start for the next iteration using the second largest value of σ. As long as the algorithm progresses as the value of σ is decreased contributing in the generation of the new estimate signal. As shown in Fig. 9 [78], the value of σ decreases the alternative function approaches the $F(x)$ in case of ℓ_0-norm.

Over the past few years several relaxation algorithms have been proposed to approximate the aforementioned problem under condition

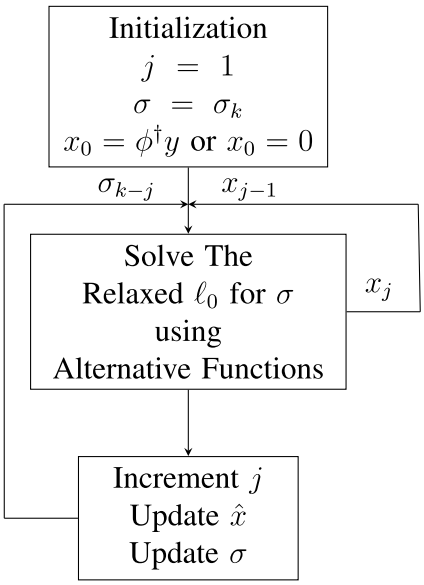

Fig. 8. Relaxation algorithms mechanism.

Algorithm 8: WReSL0 and GPL0

Input: measurement matrix ϕ, compressed signal y, and maximum sparsity K
Output: original sparse signal x
Initialize: $j = 0$, estimate vector $x_0 = \phi^{\dagger} y$, decreasing parameter $\sigma = [\sigma_1 \sigma) 2 \dots \sigma_k]$, gradient descent step γ
while $j < K$ **do**
  1) Update $\sigma_j = \sigma_k$ and $\hat{x} = \hat{x}_{j-1}$
  In WReSL0:
    2) Calculate the gradient:
      $d = \frac{\sigma}{2\gamma}(e^{\frac{-|x|}{\sigma}})^T(\frac{2\gamma x\sigma^2}{(\gamma x^2+\sigma^2)^2})$
  In ℓ_0-GP:
    2) Calculate the gradient:
      $d = (\phi^T(\phi x - y)) + 2\lambda[\frac{x_1\sigma}{(x_1^2+\sigma)^2} \dots \frac{x_j\sigma}{(x_j^2+\sigma)^2}]^T$
  3) Update the gradient direction: $\beta_j = \hat{x}_{j-1} - \gamma d$
  4) Constrained orthogonal projection: $\hat{x_j} = \beta_j - \phi^T(\phi\beta_j - y)$
  5) Update $\hat{x_j} = \hat{x}$
  6) Increment j
end

where the input signal x is sparse enough and the RIP is satisfied. The proposed algorithms implement the alternative functions by finding either ℓ_1 or ℓ_2-norms.

The Basis Pursuit (BP) was first introduced in [79], where the ℓ_0-norm in (15) is relaxed to be ℓ_1-problem, as shown in the following equation which is solved by Linear Programming (LP) method.

$$\min_{x} \|x\|_1 \quad s.t. \quad \phi\underline{x} = \underline{y} \tag{20}$$

The Gradient Projection (GP) is another family of relaxation algorithms, where the smoothing of the ℓ_0-norm is performed using ℓ_2-norm. Several variations of this relaxation method have been proposed in the literature. The work in [78] proposed the GP ℓ_0-norm (GPL0), where the Lagrangian is associated with the iterative gradient method to conclude a smoothing function similar to $R_2(x)$. The authors in [80] proposed the Weighted Regularized Smoothed ℓ_0-norm minimization (WReSL0) algorithm with a smoothing function similar to the $R_1(x)$ in (18), where the new technique is used to solve the UBSS problem. Both algorithms are illustrated in details in Algorithm 8. The complexity of both algorithms is $O(K)$.

Table 1
Comparison between reconstruction algorithms.

Algorithm	Family	Complexity	Recovery time
OMP	Greedy	$O(MNK)$	Fast
StOMP	Greedy	$O(MNK)$	Fast
MP	Greedy	$O(MN)$	Fast
SMP	Greedy	$O(MNK)$	Fast
CoSaMP	Greedy	$O(MN)$	Moderate
IHT	Greedy	$O(MN)$	Moderate
SAMP	Greedy	$O(MNK)$	Fast
BP	Relaxation	$LP(M, N)$	Slow
GP	Relaxation	$O(K)$	Slow

Algorithm 9: BCS-Smoothed Projected Landweber (BCS-SPL)

Input: measurement matrix ϕ_B, transformation matrix ψ, compressed signal y, maximum sparsity K, and total number of BCS-blocks B
Output: original sparse signal x
Initialize: loop variable $j = 0$, block index $b = 0$, estimate vector $x_0 = \phi^T y$, and error $E_0 = 0$
while $j < K$ *or* $|E_j - E_{j-1}| < \epsilon$ **do**
  1) Noise removal and signal enhancement:
    $F_j = Weiner(x_j)$
  while $b < B$ **do**
    2) Projection on convex set:
      $G_{j_b} = F_{j_b} + \phi_B^T(y - \phi_B F_{j_b})$
  end
  3) Transformation into certain domain: $H_j = \psi G_j$
  4) Choose the largest elements in H_j and ignore the rest.
  5) Reversing the transformation: $\hat{x}_j = \psi^{-1} H_j$
  while $b < B$ **do**
    6) Projection on convex set:
      $\hat{x}_{j+1_b} = \hat{x}_{j_b} + \phi_B^T(y - \phi\hat{x}_{j_b})$
  end
  7) MMSE calculation: $E_j = ||\hat{x}_{j+1} - \hat{x}_j||_2$
end

The authors in [81] derived a mathematical proof showing that the number of measurements needed for recovering sparse signal x using OMP is $O(K\ln(N))$, where K is the number of non-zeros in signal x of N length. The authors added that the OMP is still easier and faster than the Basis Pursuit (BP). Table 1 shows a comparison of most commonly used reconstruction algorithms in the literature. Comparison is performed with respect to computation complexity and time taken by the algorithm to reconstruct the signal.

3.6.2. BCS reconstruction algorithms

Dealing with 2D natural signals, BCS is the best approach to be used. Fig. 10 shows the variations done in the literature developing reconstruction algorithms for BCS.

The TV reconstruction algorithm [53] used for 2D signals requires heavy computations, which makes it impractical in case of CS systems. To overcome this dilemma, the authors in [26] proposed a new reconstruction algorithm associated with BCS entitled Smoothed Projected Landweber (SPL). The algorithm starts by applying $z \times z$ Weiner filter for noise reduction and smoothing the signal. The algorithm proceeds by applying three extra steps on the smoothed signal, as shown in Algorithm 9. First, projecting each block of the smoothed signal onto convex set S. Second, applying Hard Thresholding (HT) by transforming the resulting signal into certain sparse domain; selecting the largest elements only; then inverting the transformation. Third, the signal is projected back to the convex set S. The algorithm then loops until either reaching the maximum sparsity K or error E is less than ϵ.

Several papers have developed the aforementioned algorithm to reconstruct the BCS signals by varying multiple steps to gain better

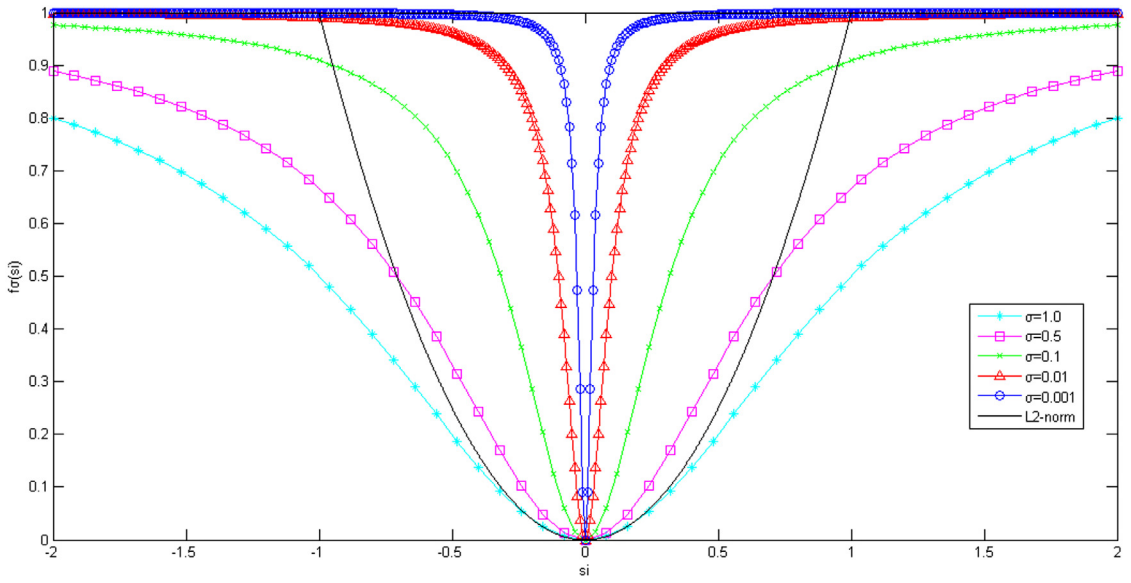

Fig. 9. Relaxation functions curve [78].

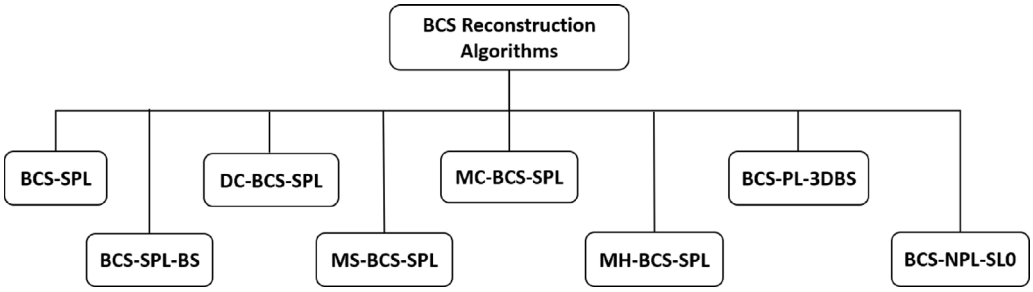

Fig. 10. BCS reconstruction algorithms types.

performance, speed, or simplicity. The authors in [26] used the Lapped Transform (LT) instead of the wavelet transform, due its orthogonal properties and low computation complexity that is not available in the wavelet transform except in the Haar basis. The authors showed by results that the performance of the proposed algorithm is similar to the BCS-TV.

In [82], the Bivariate Shrinkage (BS) is adopted in association with contourlet transform and complex valued dual tree wavelet transform due to their multi-scale directional decomposition structure to provide sparsity enforcing thresholding. The proposed algorithm is entitled BCS-SPL-BS. Simulation results show that the proposed algorithm obtains better performance compared to the BCS-TV.

The Disparity Compensated SPL (DC-SPL) proposed in [83] aims to improve the performance of the algorithm by considering disparity information at the reconstruction. Results compare the performance of the proposed algorithm with the direct BCS-SPL using different directional transforms such as: DCT, DWT, CT, and Dual-tree Discrete Wavelet Transform (DDWT). It has been shown that both direct BCS-SPL as well as DC-BCS-SPL with the DDWT achieve the best performance at both low and high sub-rates.

Multiscale BCS-SPL (MS-BCS-PSL) is illustrated in [84], where direct BCS-SPL is deployed in discrete wavelet domain, where the signal is decomposed into levels and sub-bands, then into blocks. The main contribution of the algorithm is reducing the reconstruction time and enhancing the PSNR compared to Gradient Projection for Sparse Reconstruction (GPSR), TV, and direct BCS-SPL.

For the sake of video reconstruction, two algorithms were proposed in [85,86] entitled Motion Compensated BCS-SPL (MC-BCS-SPL) and Multi-hypothesis BCS-SPL (MH-BCS-SPL) respectively. The MC-BCS-SPL aims to reconstruct the residual between the current frame and its motion compensated prediction. The MH-BCS-SPL takes into consideration both spatial and temporal correlation to enhance signal reconstruction. Results has showed the performance enhancement compared to direct BCS-SPL applied on stationary images.

Since in many practical applications Weiner filtering tends to destroy fine details and blur the sharp edges of the signal, the smoothing operation is removed in [87]. The algorithm deploys 3D-Bivariate Shrinkage (3DBS) associated with soft-thresholding step replacing the conventional hard thresholding step for better noise variance estimation. The 3D Wavelet Packet Transform (3D-WPT) is used to compare with the state of art. Simulation results show the performance enhancement compared with BCS PL-2DBS associated with 2D-DDWT.

The authors in [88] introduced a new algorithm entitled BCS Robin Monro (BCS-RM), a stochastic approximation algorithm to reconstruct DPCM-BCS encoded signals. Simulation results show that the new approach achieves better PSNR compared to the BCS-SPL.

A new approach combining the benefits of both BCS-SPL and SL0 entitled (BCS-NPL-SL0) is proposed in [89] reducing the construction time and achieving better performance. The algorithm replaces the simple thresholding mechanism with Lagrangian calculation as in SL0 which leads to higher computation complexity.

4. State of art

Table 2 lists all the proposed matrices in the related work and compares the deployed system in each paper. The matrix type refers to the type of the constructed measurement matrix ϕ either random or deterministic. The entry type represents the type of elements building

Table 2
Comparison between measurement matrices in the literature.

Algorithm	Matrix type	Entry type	RIP/ incoherence	Noise resilience	K & M relationship	Memory cost	Computation complexity	Decoding algorithm
GRM	Random	Float	Yes	Yes	$M \leq K \log \frac{N}{K}$	High	$O(MN)$	Multiple Algorithms
[41]	Random	Float	Yes	Yes	$K \leq \sqrt{M} e^{\frac{1}{M}}$	High	$O(MN)$	OMP
[57]	Deterministic	Float	RIP-1& RIP-2	Yes	$M \leq K \log \frac{N}{K}$	Medium	$O(N \log \frac{N}{K})$	Linear Programming
[61]	Deterministic	Complex	StRIP	Yes	$M \leq k \log N$	Medium	$O(k^2 \log^2 N)$	Not Mentioned
[62]	Deterministic	0 & ±1	StRIP	Yes	$M \geq K \log_2(1 + \frac{N}{K})$	Low	$O(2^{m(m+1)})$	Reed Muller Functions
[63]	Deterministic	Complex	StRIP	Yes	$M \leq \frac{1+\sqrt{K}}{2}$	High	$O(N \log N)$	Chirp Decoder
[64]	Random	Float	StRIP	No	$K \leq \frac{M}{\log \frac{N}{K}}$	Low	$O(MN)$	Linear Programming
[65]	Deterministic	Float	StRIP	Yes	$k \leq C_0 \frac{M}{\log N}$	Medium	$O(N + M - 1)$	ℓ_1-LS, SP & SAMP
[66]	Random	Float	Tabulated	No	Not Mentioned	Low	$O(M + N)$	OMP
[90]	Random	Complex Binary	$\mu = 1$	Yes	$M \leq K \log N$	Medium	$O(N \log N)$	Not Mentioned
[91]	Random	0, ±1 with SF	RIP-3	Yes	$K \leq M^3 \ln(\frac{N}{M})$	Low	$O(N)$	GP
[92]	Deterministic	Binary	Not Mentioned	Not Mentioned	$M = K2^{O(\log \log N)^E}$	Low	$O(kN2^{(\log \log N)^E})$	Not Mentioned
[93]	Random	0 & Complex	Yes	Yes	$M \geq K \log N + \log^3 N$	Medium	$O(N)$	Not Mentioned
[94]	Random	Complex	StRIP	No	$M \geq Ck \log(1 + \frac{N}{M})$	Medium	$O(N)$	OMP
[95]	Deterministic	Binary	$k \leq max(M^{\epsilon/2^{d-1}}, M^{\frac{1}{9d^2 \log d}})$	Yes	$K \leq \frac{1}{\sqrt{M}}$	Low	$O(mrp)$	BP
[96,97]	Random	Float	StRIP	No	$k \leq \frac{cM}{\log(\frac{N}{k})}$	Medium	$O(MN)$	OMP
[98]	Deterministic	Integer	$k < \frac{p}{r} + 1$	Not Mentioned	$k \leq \frac{\sqrt{M} \log M}{\log \frac{N}{M}}$	Medium	$O(p^{r+3})$	Not Mentioned
[99]	Random	Float	$\mu \leq \sqrt{\log(\frac{N}{r})}$	No	$M = \frac{KN}{r} \log(N) \log(\frac{N}{c})$	Medium	$O(MN)$	GPSR
[100]	Random	Float	RIP-3	No	$M \geq Ck^3 \ln(\frac{N}{k})$	Medium	$O(N + M - 1)$	TV
[101]	Random	±1	Not Mentioned	No	$M \geq (K\sqrt{\frac{N}{B}}(\log N)^2)$	Low	$O(N \log B)$	ℓ_1 minimization, TV & IHT
[102]	Random	Float	StRIP	No	$M > C \log^3 N$	Medium	$O(N \log N)$	Not Mentioned
[103]	Deterministic	Complex	$\mu \leq \frac{\sqrt{M}+2}{M}$	No	$K \leq \frac{1}{2}(1 + \frac{M}{\sqrt{M}+2})$	High	$O(pMl - pM)$	OMP
[103]	Deterministic	Complex	$\mu \leq \frac{\sqrt{M+1}+3}{M}$	No	$K \leq \frac{1}{2}(1 + \frac{M}{\sqrt{M+1}+3})$	High	$O(M(p^r - 1)(l - 1))$	OMP
[104]	Deterministic	Complex	$\mu \leq \frac{d-1}{M}$	No	$K \leq \frac{1}{2}(1 + \frac{\sqrt{M} \log M}{\log(\frac{N}{M})})$	High	$O(p^{2mh})$	BP
[105]	Deterministic	Integer	$k \leq D(\frac{p}{r} + 1)$	No	Not Mentioned	Medium	$O(p^{r+3})$	OMP
[106]	Random	Binary	$\mu \leq \sqrt{\frac{NL}{M\beta}}$	No	$K \leq \frac{L}{M}$	Low	$O(LN)$	GPSR & TV
[107]	Deterministic	±1	$k \leq 2^j + 1$	Yes	$M \leq k(\log_2 N)^{\frac{\log_2 k}{\ln \log_2 k}}$	Low	$O(MN)$	MP
[108]	Deterministic	Complex	$\mu \leq \frac{p(p^{l-r}-1)}{2(p-1)(p^l-1)}$	Yes	$M \leq k_{gr}(\log_p N)^{\frac{\log_p k_{gr}}{\log_p \log_p k_{gr}}}$	High	$O(p^{1/r((l-1)(l-r)\log_p r)})$	OMP
[109]	Deterministic	Binary	$k < \frac{2^r + 2^{1+\frac{r}{2}}}{s+1}$	Yes	$K \leq \frac{(\sqrt{M}+\sqrt[4]{M}) \log M}{2 \log N}$	Medium	$O(2^{r(s+2)} + 2^{sr/2}(1+3r))$	OMP
[110]	Random	Float	$\mu \leq C\sqrt{\log N}$	Yes	$\mu \leq C\sqrt{\log N}$	Low	$O(\sqrt{\log N})$	FPC-AS
[111]	Random	Float	RIP	No	$M \geq \log \frac{N}{K}$	Medium	$O(\frac{MN}{n_{Blocks}})$	ℓ_1 minimization
[112]	Deterministic	Binary	$\mu = \frac{1}{r}$	No	$k \leq M$	Low	$O(rq^3)$	OMP
[113]	Deterministic	Float	$\mu \leq \frac{1}{q+1}$	No	$k = \frac{M}{\log N}$	Medium	$O(\frac{1}{\sqrt{M}})$	CoSaMP
[114]	Deterministic	Complex	$\mu \leq \frac{1}{q}$	Yes	$k \leq \sqrt{M}$	Medium	$O(q^5)$	OMP

(*continued on next page*)

Table 2 (*continued*).

[115]	Deterministic	Binary	$k \leq q+1$	Yes	$K \leq \sqrt[3]{M}$	Low	$O(q^7+q^6+q^5+q^4+q^3+q^2+q)$	OMP
[115]	Deterministic	Binary	$k \leq q$	Yes	$K \leq \sqrt[3]{M}$	Low	$O(q^7+q^6+q^4)$	OMP
[115]	Deterministic	Binary	$k \leq q+1$	Yes	$K \leq \sqrt[3]{M}$	Low	$O(q^5-q^6+q^4-q^3+q^2+q)$	OMP
[115]	Deterministic	Binary	$k \leq \left\lfloor \frac{q+1}{2} \right\rfloor$	Yes	$K \leq \sqrt{M}$	Low	$O(q^5+q^3+q)$	OMP
[116]	Deterministic	Integer	No	Yes	Not Mentioned	Low	$O((p-1)^2)$	OMP
[117]	Deterministic	Float	StRIP	Yes	$M \leq K^3 \ln(\frac{N}{K})$	Medium	$O(N)$	OMP
[118]	Deterministic	Float	$k \leq \frac{3+\sqrt{q}}{2}$	Yes	Not Mentioned	High	$O(q^2+q)$	LASSO
[119]	Deterministic	Binary	Plotted Not Formalized	No	$K \leq \frac{M}{1.5 \log N}$	Low	$O(N+M-1)$	New Technique
[120]	Deterministic	Binary	$k \leq l+1$	Yes	$K \leq \frac{M}{\sqrt{N}}+1$	Low	$O(lr^3)$	OMP
[121]	Deterministic	Binary	$k \leq \frac{p_2}{r}+1$	Yes	$M \leq Ck(\log_2 N)^{\frac{\log_2 k}{r n(\log_2 k)}}$	Low	$O(p_2(p_1 p_2)^{r+2})$	OMP
[122,123]	Random	Float	StRIP	Not Mentioned	$M \leq K \log \frac{N}{K}$	High	$O(MN)$	OMP & BP
[124]	Deterministic	Float	Not Mentioned	No	$M \leq k \log N$	Low	$O(N \log N)$	NESTA
[125]	Random	Float	RIP-0	Yes	$M \leq K$	Medium	$O(N)$	Not Mentioned
[126]	Deterministic	Binary/Float	Plotted Not Formalized	No	Not Mentioned	Low/ Medium	$O(MN)$	OMP
[127]	Deterministic	Integer	Yes	Yes	Not Mentioned	Medium	$O(MN)$	OMP
[128]	Deterministic	Float	Not Mentioned	Yes	$M \leq K \log N$	Medium	$O(N \log N)$	ℓ_1 minimization & TV
[129]	Deterministic	Binary	Tabulated μ	Yes	$K \leq O(\sqrt{\frac{M}{\log M}})$	Medium	$O(MN)$	OMP
[130]	Random	Binary	Yes	Yes	Not Mentioned	Low	$O(MN)$	OMP

the ϕ matrix. The third column represents how far the proposed matrix satisfies the RIP. The relation of mutual coherence μ with the sparse signal metric K is listed if present. Most of the papers in the literature studied the effect of AWGN on the compression mechanism showing how far their proposed approach is immune to noise. The relation between the sparse signal metric K and the measurement matrix size M is studied as well. Since the motivation of this survey is to find the most convenient type of CS to be implemented on physical hardware, the memory cost is studied based on the type of elements of measurement matrix ϕ, the reconstruction algorithm, and the computation complexity.

The authors in [90] proposed a complex noiselet system constructed using ψ as Haar wavelet matrix and ϕ as an orthogonal noiselet matrix which results in mutual coherence $\mu = 1$. The authors mentioned that the matrix is hardware friendly as the elements are binary complex elements. The paper presented the reconstruction of certain image but did not mention which reconstruction algorithm is used.

Toeplitz and Circulant matrices are studied in [91], where a mathematical proof is provided that both matrices are satisfying the RIP of order $3m$ with high probability. Since the proposed matrices lack universality unlike the random Gaussian matrix, the authors showed that they are able to recover signals that are either Piecewise Constant (PWC) or sparse in the Haar wavelet domain. Results show that proposed matrices have similar recovery performance compared with the random Gaussian matrix. The authors noted that the matrices are hardware friendly and require small memory storage as decoding is performed using the FFT.

The proposed matrix in [92] is constructed using a small family of hash functions implemented using extractor graphs. The size of the matrix is $k2^{O(\log\log N)^E} \times N$, where E is a constant number larger than 1. The paper did not show any details about neither universality nor RIP.

Romberg in [93] proposed a measurement matrix based on random convolution that is universal and satisfies the RIP. Since the matrix is complex diagonal one, the author mentioned that the construction of matrix ϕ can be done using random demodulator that consists of multiplier and integrator. The recovery is performed using ℓ_1-minimization with probability $1 - O(\frac{1}{N})$.

In [94], partial orthogonal symmetric Toeplitz matrix is proved to satisfy Statistical RIP (StRIP). The paper mentions that the proposed matrix requires small memory storage and easily implemented. Simulation results are deployed on sparse signals in time and DCT domains. Using OMP in signal reconstruction, the proposed matrix performance is similar to the Hadamard matrix and better than the Bernoulli Toeplitz matrix in both domains.

The authors in [95] established a deterministic matrix formed by selection of rows of Fourier matrix satisfying the RIP of order $k \leq max(M^{\epsilon/2^{d-1}}, M^{\frac{1}{9d^2 \log d}})$, where $0 < \epsilon < 1$ and d is the degree of the polynomial used to generate the set of rows to be selected. The matrix size is $m \times rp$, where p is large prime number and r is integer satisfying $r \geq 1$. The complex Basis Pursuit solver is used in signal recovery to measure the reconstruction performance.

Aside from Gaussian random matrices, Bernoulli distribution is investigated in [96,97], where four types of random matrices are proposed:

- Random symmetric signs matrix: where elements are distributed with the following formula:

$$\phi_{ij} = \begin{cases} \frac{1}{\sqrt{M}} & with\ probability\ 1/2 \\ \frac{-1}{\sqrt{M}} & with\ probability\ 1/2 \end{cases} \tag{21}$$

The authors proved that for $k \leq cM/\log(N/k)$, where c is a constant, the RIP property is satisfied with probability $P \geq (1 - 2\exp^{-cM})$.

- Hadamard matrix: where rows of the matrix are selected from $N \times N$ Hadamard matrix with restriction $N = 2^q$, where q is a positive integer.
- Random binary matrix: where elements are distributed according to the following formula:

$$\phi_{ij} = \begin{cases} \frac{2}{\sqrt{M}} & with\ probability\ 1/2 \\ 0 & with\ probability\ 1/2 \end{cases} \quad (22)$$

It is proved that for $k \leq cM/\log(N/k)$, the RIP property is satisfied with probability $P \geq (1 - 2\exp^{-cM})(1 - 2^{-M})$.

- Semi-Hadamard matrix: is a special kind of binary matrix. Assuming that h_{ij} is the ith row and jth column in partial Hadamard matrix, the new matrix is generated by deleting all negative numerical values to follow the following distribution:

$$\phi_{ij} = \begin{cases} \frac{2}{\sqrt{M}} & h_{ij} = 1 \\ 0 & h_{ij} = -1 \end{cases} \quad (23)$$

The reconstructed signal is required to be sparse in frequency domain. The OMP is used in signal recovery. Simulation results show that the performance of the proposed matrices is similar to the Gaussian random matrix with the benefit of less storage. The paper did not give any details about the encoding and decoding complexity.

In [98], DeVore used polynomials over finite fields to build up a measurement matrix of size $p^2 \times p^{r+1}$, where p is a prime number and r is an integer that lies within the following range $0 < r < p$. The RIP of the proposed matrix is of order $k < \frac{p}{r} + 1$, and the coherence is given by $\mu \leq \frac{r}{p}$. Since the matrix structure is circulant, it is considered to be memory friendly. Neither universality, nor noise is discussed in the paper. The coherence is lower bounded by Johnson bound not the Welch bound [55]. The author main goal was to maximize the RIP order of the constructed matrix, so the paper did not give any details about the complexity of either encoding or decoding.

The authors in [62] constructed a deterministic measurement matrix based on the second order Reed–Muller functions. Although the paper did not give any indication about the memory cost, the constructed matrix can be considered hardware friendly due to its diagonal structure of size $2^m \times 2^{m(m+1)/2}$, where the number of measurements is $M = 2^m$.

Thong et al. in [99] were the first to investigate the usage of SRM as a measurement matrix in CS. The proposed SRM is defined as orthonormal matrix whose columns are permuted randomly or signs are reversed with the same probability. The proposed matrix has three main advantages. First, Universality, as it is incoherent with a variety of orthonormal matrices except the identity matrix. Second, the number of measurements required for exact reconstruction is nearly optimal. Third, low complexity and fast computation.

The calculated probabilistic mutual coherence is $\mu \leq \sqrt{\log(\frac{N}{r})}$, where r is the number of non-zero elements in ϕ matrix. The former relation is valid provided that $M = \frac{KN}{r}\log(N)\log(\frac{N}{c})$ and $M = k + \frac{N\sqrt{k}}{r}\sqrt{\log^3(N)}$ for reconstruction of uniform and non-uniform sparse signals respectively. The chosen basis matrix ψ is the wavelet transform. The used reconstruction algorithm is the ℓ_1-LP solver based on the GPSR. Simulation results show that the proposed matrix performance is similar to the Haar matrix, the DCT matrix, sparse FFT matrix, and Brute Force (BF) method using partial FFT.

Toeplitz matrix proposed in [100] is used as the measurement matrix for medical imaging applications as MRI. The paper showed that the proposed matrix satisfies RIP-3, when $M \geq Ck^3\ln(\frac{N}{k})$. Since MRI images are usually sparse in the wavelet domain, TV is used as the reconstruction algorithm.

In [101], scrambled block Hadamard matrix is proposed due to its sparsity, small memory size, fast computation, and easy implementation in the optical domain. The structured matrix is generated by multiplying scrambled operator with group of $B \times B$ Hadamard matrices concatenated diagonally to form $N \times N$ matrix. The adopted scrambling operators are: Randperm MATLAB® method, Linear Congruential Permutation (LCP), and Row Permutation and Row Inversion (RPRI). In order to measure the performance of the proposed matrix, ℓ_1-optimization, min-TV, and iterative thresholding are used. Results show that associating the iterative thresholding decoder with the LCP scrambler achieves the best performance for the proposed matrix. The matrix is universal with any ψ.

The authors in [131] were the first to use the chaotic sequences with CS to design a deterministic measurement matrix. The main purpose of the paper was to construct a chaos filter generated by the logistic map for CS that has the same structure as random filters except that the filter tap values are generated by deterministic chaos instead of random variables. The proposed matrix that has a banded quasi-Toeplitz structure is of size $(N + L - 1) \times N$, where L is the filter length and N is the signal length. OMP is used in reconstruction. The paper presents performance comparison between random and chaotic filters showing that the later has better recovery performance. There is no indication about neither the RIP nor the mutual coherence.

Since there is no practical algorithm verifying whether the measurement matrix satisfies the RIP or not, the authors in [61] proposed a relaxed version of RIP called StRIP. The work generalized the proposed matrices in [62,63] by showing that those matrices satisfy the StRIP. The authors showed that using the relaxed version of the RIP will reduce the number of required measurement M. Partial Fourier ensemble was used to prove the above property, where the M has been reduced from $k\log^6 N$ to $k\log N$.

The chirp sensing codes proposed in [63] are used to construct the measurement matrix of size $M \times M^2$ and enable easy decoding. The chosen matrix satisfies the StRIP. The memory cost is considered high due to the complex entries of the measurement matrix. Also, the universality is not discussed in this paper.

The authors in [102] proposed a new type of SRM, where the matrix is generated by multiplying three matrices $\phi = \sqrt{\frac{N}{M}}DFR$. The D Matrix is $M \times N$ diagonal binary random matrix, the F Matrix of size $N \times N$ is an orthonormal matrix, such as FFT, DCT, and WHT, and the R Matrix, which are $N \times N$ diagonal matrix whose diagonals follow Bernoulli distribution. The paper gives a mathematical proof on how the matrix satisfy the StRIP. Results compare the distortion rate of the proposed matrix with the random Gaussian matrix showing that both nearly have the same distortion rate. The proposed matrix has low complexity of $O(N\log N)$ and the number of elements need to be stored is $O(N)$. The paper did not give any indication about the deployed decoding algorithm.

The link between chaotic sequences and CS is discussed in [64], where the constructed matrix is proved to satisfy the StRIP. LP in SparseLab is used in signal recovery. Simulation results show that the recovery performance of such matrix is nearly equal to the random Gaussian and random Bernoulli matrices.

In [103], the proposed measurement matrix is constructed via multiplicative character sequences. The two proposed matrices are: matrix based on power residue sequences of size $p \times M(l-1)$, where p is a prime number and l is a divisor of $p - 1$. The second one is matrix based on sidelnikov sequences of size $p^r - 1 \times M(l-1)$, where r is a positive integer number.

Using the OMP in the reconstruction, Yu mentioned that their proposed matrices theoretically were unable to overcome the deterministic bound $K \leq \sqrt{M}$. However, the author showed that numerical results give more promising proof to be $K \leq \frac{M}{\log N}$. The computation complexity of the proposed matrices was said to be low due to the circular nature of the used sequences, but since the elements are complex this adds more storage cost. The paper lacks any comparison with the literature.

Yu extended his work in [104] and proposed another measurement matrix constructed based on additive character sequences of size

$p^m \times p^{mh}$, where p is an odd prime number, m, and h are positive integers where $h > 1$. This time the author used the basis pursuit to compare the recovery performance of the proposed matrix with the chirp matrix [63] and the random partial Fourier matrix.

The authors in [65] proposed an Orthogonal Symmetric Toeplitz Matrix (OSTM) satisfying StRIP. The proposed matrix is better than the matrices proposed [61,93] due to the Toeplitz structure that provided smaller memory storage and fast recovery technique, as the implementation is based on FFT. The deployed recovery algorithms are ℓ_1-regularized Least Squares (ℓ_1-LS), SMP, and SAMP. Simulation results show that the recovery performance of the OSTM is similar or better than Gaussian matrix, random partial Walsh–Hadamard matrix and random partial DCT matrix.

The proposed matrix in [105] is a structured diagonal matrix of size $D \times D$, where each element in the diagonal is a polynomial deterministic matrix. The size of the later matrix is $p^2 \times p^{r+1}$, where p is a prime number and r is an integer defined by the range $0 < r < p$. The authors have mentioned that the matrix is easily implemented on hardware. The OMP was used in signal recovery. Results show the improvements appearing due to the use of the proposed matrix compared to the ordinary measurement polynomial matrix.

The authors in [106] presented a Binary Permuted Block Diagonal (BPBD) matrix. The matrix is constructed by concatenating PBD submatrices with total size equals to $LK \times K$, where L is chosen to be small as possible to achieve low mutual coherence and K is the number of diagonals in the sub-matrix. The calculated mutual coherence is $\mu \leq \sqrt{\frac{NL}{M\beta}}$, where $0 < \beta < 1$. Simulation results are presented by using GPSR ℓ_1-minimization solver [132], and the TV minimization solver to compare the recovery performance of the proposed matrix with the Scrambled Fourier (SF) matrix, the Partial Noiselet (PN) matrix, and the Scrambled Block Hadamard (SBH) matrix. The authors mentioned that the matrix is hardware friendly and require small storage due to its structured nature.

In [133], the work has been extended to prove that the diagonal matrices satisfy the RIP when the following condition is valid: $M \geq \mu^2 K \log^2(K) \log^4(N)$. The proposed work in [107] establishes a connection between the optical codes and binary measurement matrices. The authors proposed two matrices:

- The first matrix is constructed using the Bose, Chaudhuri, and Hocquenghem (BCH) code of size $2^l - 1 \times 2^{O(2^{\frac{(l-j)\ln j}{j}})}$ satisfying the RIP of order $k \leq 2^j + 1$, where $l = \lceil \log_2 k \rceil$ and j is an integer lies between $1 < j < N$. The calculated mutual coherence is $\mu \leq \frac{2^{l-j}-1}{2^l-1}$. Since the BCH codes are subset of cyclic codes, the authors used this property to construct a circulant matrix to reduce the computation and memory complexity. In signal recovery, the adopted MP is implemented using FFT and IFFT based on the matrix circulant structure.
- The second one is a ternary matrix created by combining the binary and bipolar matrices to form a matrix of elements $\{0, \pm 1\}$. The size of the matrix is $p^2 \times 2^{O(r^{\frac{ln(\log_2 p - \log_2 r)}{\log_2 p - \log_2 r}})} p^{r+1}$, where p and r are the same variables used in [98]. The main contribution of this matrix is that the order N columns in the measurement matrix is larger than Devore matrix [98].

Simulation results has showed that the BCH matrix outperforms the ternary, Devore, and random matrices when measuring the probability of perfect recovery with respect to k.

The main drawback in all constructed matrices in the work listed earlier is that their explicit construction is only known for size $M \times N$, where $\frac{N}{M} \leq 2$. Furthermore, even for low RIP orders, increasing the bound of N is quadratic with respect to M. Only Devore's matrix [98] and BCH matrix [107] provided RIP without this restriction.

The authors in [134] were the first to present a mathematical connection between Channel Coding Linear Programming Decoding (CC-LPD), and CS Linear Programming Decoding (CS-LPD) known as Basis Pursuit (BP). The measurement matrix was viewed as binary parity-check matrix. They provided the first deterministic construction of CS matrices with an order optimal number of rows using high-girth LDPC codes constructed by Gallager. However, due to the unstructured nature, both R-SBM and sparse matrices constructed by Gallager are difficult to implement in hardware though they often obtain good sensing performance.

The work on the BCH codes in [107] is extended in [108] to construct another measurement matrix of size $p^{l-1} \times p^{O(\frac{(l-r)\log_p r}{r})}$ whose elements are complex, where l is an integer number $l > 1$, p is a prime number, and r is defined by the following range $1 \leq r \leq l-1$. The k_{gr} defined in the M inequality is calculated by $k_{gr} = \left\lfloor \frac{1}{2} + \frac{(p-1)(p^l-1)}{p(p^{l-r}-1)} \right\rfloor$. The mutual coherence of the matrix is defined as $\mu \leq \frac{p(p^{l-r}-1)}{2(p-1)(p^l-1)}$. The relations in [107] is special case when $p = 2$. The memory cost is considered high due to complex matrix elements. Using the OMP as recovery algorithm, simulation results show that the recovery percent of the modified BCH matrix is better than the Chirp matrix [63], complex Gaussian matrix, and the random DFT matrix.

The authors in [109] generalized the work done by Devore in [98] by constructing a binary measurement matrix based on algebraic geometry curves. The two constructed matrices are based on two well known curves. The first one is elliptic curves, which are well known by their usage in cryptography. The constructed matrix is of size $(2^{2r} + 2^{1+\frac{3r}{2}}) \times 2^{sr}$, where s is an integer defined in this range $(1 \leq s < 2^r + 2^{\frac{r}{2}+1} + 1)$. The RIP of order $k < \frac{2^r + 2^{1+\frac{r}{2}}}{s+1}$ is satisfied, and the mutual coherence is $\mu \leq \frac{s}{2^r + 2^{\frac{r}{2}+1}}$. The second one is the Hermitian curves, where the proposed matrix is of size $q^{5/2} \times q^{\frac{s+1-q+\sqrt{q}}{2}}$, knowing that q is a prime number, and s is an integer lying between $(q - \sqrt{q} - 1) \leq s \leq q^{3/2}$. The matrix satisfies RIP of order $k \leq 1 + \frac{q^{3/2}}{s}$ and the calculated mutual coherence is $\mu \leq \frac{s}{q^{3/2}}$. The OMP is used in signal recovery. Results show that the elliptic matrix outperforms the recovery rate the Gaussian matrix. The coherence of the hermitian matrix is shown to be better than Devore.

In [110], the authors proposed Partial Golay-Paired Hadamard (PGPH) matrix due to its fast computation on sparse signals in time, FFT, and DCT domains. The proposed matrix is a good alternative to partial FFT and Walsh–Hadamard as the later are only applicable on sparse signals in time domain only. The generation of the matrix is similar to the SRM except for the substitution of the random diagonal matrix with a deterministic one. The matrix is shown to satisfy the mutual coherence $\mu \leq C\sqrt{\log N}$ under the conditions of $M \geq Ck \log^5 N$ and $M \geq Ck \log^2 N$ for reconstruction of uniformly and non-uniformly sparse signals respectively. The Fixed Point Continuation and Active Set algorithm (FPC-AS) for solving ℓ_1-regularized least squares problem [135] is deployed. Simulation results show that the proposed matrix performance is near to the random Gaussian matrix and better than the partial Fourier and partial Walsh Hadamard matrices.

After studying symmetric block diagonal matrix in [26] and the block diagonal sampling matrix in [133], the proposed matrix in [111] is a mix of both types to generate a generalized asymmetric structured block diagonal matrix offering the flexibility and applicability in practical communication systems. The authors proved that the proposed matrix satisfy the RIP. The reconstruction technique used is not mentioned. Simulation results compare the performance of dense random matrix, symmetric, and asymmetric matrices. The paper noted that the matrix requires small memory storage.

In [136], a min–max condition for mutual coherence was derived so that the matrix shall be constructed based on that condition. The work in [137] proposed the construction of measurement matrix using Grassmannian matrix as it provides a mutual coherence near the Welch bound. The MATLAB® built-in function "mrdivide()" is used to generate the matrix. Hadamard and DCT matrices were the two initial points to construct the Grassmannian matrix. The paper did not compare the results with any of the state of art.

Since the constructed matrix form LDPC codes need high storage and high decoding complexity due to the randomness structure. The authors in [112] used the Quasi-Cyclic Low Density Parity Codes (QC-LDPC) to overcome these limitations with the aid of QC structure. The proposed matrix is structural matrix whose elements are circulant permutation sub-matrices. The size of the measurement matrix is $rq \times q^2$, where q is a prime number and r is defined within range $1 < r < q$. The calculated mutual coherence is $\mu = \frac{1}{r}$. With the aid of OMP, the authors showed that recovery performance is better than the random Gaussian matrix.

The cyclic shifts of binary sequences in Optical Orthogonal Code (OOC) are used to construct the proposed matrix in [113]. The matrix is multiplied with Hadamard matrix to produce a real valued matrix that takes the entries of $0, \pm 1$ before normalization. The authors constructed three matrices based on Singer construction, whose matrix size is $q^2 + q+1 \times l(q^2+q+1)$, where q and l are prime integer and integer divisible by 4 respectively. The calculated mutual coherence is $\mu \leq \frac{1}{q+1}$. The second one is Bose–Chowala construction, whose matrix size is $q^2 - 1 \times l(q^2 - 1)$ and the mutual coherence is $\mu \leq \frac{1}{q}$. The third one is Rusza–Lindstrom construction, whose matrix size is $q^2 - q \times l(q^2 - 1)$ and the mutual coherence is $\mu \leq \frac{1}{q-1}$. In order to measure the performance of the matrices, the CoSaMP algorithm is used in the reconstruction. The results show that proposed matrices have reconstruction performance better than the random Gaussian matrix.

The authors in [114] proposed a sensing matrix generated by applying the tensor product over Reed Solomon generator matrix. The size of the constructed matrix is $q^2 \times q^3$, where p is a prime number. The calculated mutual coherence is $\mu \leq \frac{1}{q}$. Using the OMP as the recovery algorithm, simulation results show that the recovery performance of the constructed matrix is better than the Gaussian matrix and nearly similar to the BCH matrix [107]. The authors mentioned that the matrix hardware implementation is easy but they did not provide any justification.

In [115], the authors use the incidence matrices of packing designs to generate binary matrices with low coherence. A series of Steiner systems, which is a kind of packing designs are obtained from finite geometry. The authors constructed four classes of binary sparse measurement matrices based on mutual coherence. Knowing that p is a prime number, the proposed matrices are the projective matrix, the affine matrix, the unital matrix, and the inverse matrix whose sizes are $(q^3+q^2+q+1) \times (q^4+q^3+2q^2+q+1)$, $(q^3) \times (q^4+q^3+q)$, $(q^3+1) \times (q^2-q^3+q)$, and $(q^2+1) \times (q^3+q)$ respectively and mutual coherence is $\mu \leq \frac{1}{q+1}$, $\mu \leq \frac{1}{q}$, $\mu \leq \frac{1}{q+1}$, and $\mu \leq \frac{2}{q+1}$ respectively.

Based on the following *Lemma*:

$$if\ C = A \odot B,\ then\ \mu(C) = \max\{\mu(A), \mu(B)\} \tag{24}$$

the authors proposed another matrices combining the pros of the binary matrices and the dense matrices to enhance the recovery performance and reduce the computation complexity and memory storage since all operations with zeros are excluded. The Hadamard and DFT matrices are merged with the four proposed matrices. Simulation results show that the recovery performance of the affine matrix outperforms the Gaussian matrix and performs equally as the BCH matrix [108]. The recovery of the inversive matrix is better than the BCH, Devore's [98], Gaussian, and algebraic curves [109]. Results also show that the combined unital and Hadamard performance is better than the Gaussian matrix and combining Devore's and Hadamard matrix. The combined protective and DFT is better than any other combined matrices with DFT. The paper only mentioned that the recovery time is small but did not formalize the consumed time in encoding and decoding process.

An extended work on the QC-LDPC codes is introduced in [116]. The proposed structural matrix is based on the multiplier group of Galois Field, where each element is either a circle permutation sub-matrix or a zero matrix. The matrix size is $(p-1) \times (p-1)^2$, where p is a prime number. The OMP is used in signal recovery and simulation results showed that the recovery performance of the proposed matrix outperformed the Gaussian and Toeplitz matrices. The paper lacks any proof for neither the RIP support nor mutual coherence.

In [117], a deterministic method is proposed to construct a Hybrid chaotic map Sparse Toeplitz structured (HcmST) matrix. Construction is performed by arranging chaotic sequence in Toeplitz structure, then sparsifying some elements selected randomly. The author has mentioned that the matrix is hardware friendly and requires low storage due to its Toeplitz-like structure and zero elements. It is proved that the proposed matrix satisfies the StRIP. The paper presents the impact of noise on signal reconstruction showing that the Mean Square Error (MSE) of the proposed matrix is low. The OMP is used in signal recovery. However, no comparison is being performed with the literature.

The matrix proposed in [118] is based on Paley graphs so that the generated Gram matrix is real valued. The size of the proposed matrix is $\frac{q+1}{2} \times q$, where q is a prime number. The mutual coherence is $\mu = \frac{2}{1+\sqrt{q}}$. For signal construction, the authors used LASSO algorithm and showed that the recovery performance of the constructed matrix is better than both real valued Gaussian matrix and the BCH matrix [107].

Since sparse matrices are hardware friendly and require low memory storage, the authors in [119] constructed a structured diagonal sparse matrix whose diagonal elements are sub-matrix in a large single row unity matrix. Regarding the universality condition, the technique requires that the transformation matrix $\psi$to be a DCT matrix. The authors did not provide a mathematical formula for the mutual coherence between the DCT transformation matrix ψ and the proposed measurement matrix ϕ. However, they added an interpolated curve between the mutual coherence and the measurements M showing that the coherence of the proposed matrix is lower than the Gaussian matrix. The paper showed that the encoding process requires $N - M$ additions without any storage requirement. A new reconstruction technique is being proposed, and results has showed that it is better than the regular OMP and the StOMP.

A graphical curve for random, Toeplitz, and circulant matrices drawing the recovery performance versus the sparsity level K is provided in [66], illustrating the trade-off between the recovery performance and matrix complexity. Since the coherence of structured matrices increases when multiplying with the basis matrix ψ, the authors proposed two scrambling methods to solve this dilemma. The first one is the predefined scrambled matrix, where the original measurement matrix is multiplied by two predefined matrices: the modification matrix and the selection matrix which work on shuffling the original elements and changing their signs to achieve better coherence. The second one is the built-in location selection, where the elements of random Gaussian matrix are stored in a memory, where an indexing function is used to access this memory. Simulation results define ψ as IDCT matrix and use the OMP in the recovery process. The paper tabulated the calculated mutual coherence of both methods and the memory storage of each matrix. It is shown that both matrices achieve optimal recovery with low memory storage. However, the second method has additional overhead due to the use of the indexer circuit.

The authors in [138] constructed a binary sparse measurement matrix based on photograph LDPC codes called Photograph LDPC Sparse Matrix (PLDPC-SM). However, there is no mathematical model provided to show neither the matrix size nor the RIP support. With the aid of the OMP, the authors were able to compare the performance of their matrix with the matrix constructed using finite geometry [115], the random Gaussian matrix, the QC-LDPC matrix in [112], and the random sparse binary matrix [139]. The results show that the proposed matrix outperforms all other mentioned matrices. Noise calculations are not taken into consideration. The structured matrix can be implemented using shift registers which makes it hardware friendly.

In [120], the authors proposed a binary measurement matrix of size $lr \times r^2$, where l and r are positive integers defined by the range $l \geq 2$ and $r \geq 3$. The mutual coherence is defined by $\mu = \frac{1}{l}$. The OMP is used to reconstruct the compressed signal and performance is compared

with Gaussian and Bernoulli matrices. The authors extended their work in [121] and constructed another binary measurement matrix of size $p_1 p_2^2 \times (p_1 p_2)^{r+1}$ with the aid of Devore method [98], where p_1, p_2 are prime numbers and r is a positive integer defined in range $r < p_2 < p_1$. The calculated mutual coherence is $\mu = \frac{r}{p_2}$. The OMP is used in signal recovery and simulation results show that the proposed matrix outperforms the Gaussian matrix in the recovery performance.

The main goal for the authors in [140] was to design a random projection measurement matrix that has small mutual coherence. The proposed matrix is constructed through concatenating two square matrices of size $M \times M$ and another sub-matrix of size $M \times N - M$ to have total size of $M \times M + N$. The mutual coherence is proved to be the minimum by using the lemma defined in (24) while constructing the measurement matrix. The construction complexity is $O(N^3)$. Both OMP and BP are used in signal reconstruction. The presented results compare the performance of the proposed matrix with [122,123].

The proposed work in [124] is paired with sparse Fast Fourier Transform (sFFT) to enable low computations at encoding and decoding compared to either convex programming or greedy methods. Simulation results show that the memory cost of the proposed matrix is better than the complex random Gaussian matrix. The NESTA algorithm proposed in [141] is used in signal recovery. The authors mentioned their work can achieve fast decoding using more flexible dictionaries without relying on adaptive sensing compared to [125].

Inspired by the matrices constructed from LDPC codes, the work in [126] proposes LDPC codes constructed from a special Balanced Incomplete Block Design (BIBD) called Bose-BIBD. Considering s is a positive integer, the authors constructed five types of matrices. The first four are hardware friendly due to binary elements. The matrices specifications are as follows:

- Type-1 matrix: of size $(12s + 1) \times (12s^2 + s)$ where $(12s + 1)$ is a prime number.
- Type-2 matrix: of size $(20s + 1) \times (20s^2 + s)$ where $(20s + 1)$ is a prime number.
- Type-3 matrix: of size $(12s + 3) \times (12s^2 + 7s + 1)$ where $(4s + 1)$ is a prime number. The generated matrix is a structured matrix of cyclic, identity, and zero sub-matrices.
- Type-4 matrix: of size $(20s + 5) \times (20s^2 + 9s + 1)$ where $(4s + 1)$ is a prime number. The generated matrix is also structured matrix of same sub-matrices.
- Modified Bose-BIBD matrix: Based on the lemma defined in (24) proved in [115], the authors multiplied the DFT matrix with the Bose-BIBD to achieve better mutual coherence. They also referred that the Grassmannian frames matrix [137] can be used as well.

The paper did not formalize the mutual coherence relationship. However, as in [119], it provided an interpolated curve comparing the mutual coherence of the proposed matrices with the random Gaussian matrix, the random sparse matrix [142], and the LDPC matrix [116] showing that the proposed matrix has the lowest mutual coherence of all. The OMP is used in the reconstruction, where the proposed four matrices are showed to have the best recovery performance for compression ratio $M/N > 1/9$. The fifth type showed that it consistently outperforms all other types of matrices but loses the simplicity of hardware implementation due to the presence of non-binary elements.

The authors in [127] used some sequence sets with optimal correlation to construct four measurement matrices based on:

- Udaya–Siddiqi sequences: The matrix size is $(2^{m+1} - 2) \times (2^{2m+1} - 2^{m+1})$ and the mutual coherence is $\mu \leq \frac{2^{(m+1)/2}+2}{2^m}$.
- Udaya–Siddiqi sequence family A: The matrix size is $(2^m - 1) \times (2^{2m} - 1)$ and the mutual coherence is $\mu \leq \frac{2^{m/2}+1}{2^m+1}$.
- Udaya–Siddiqi sequence family D: The matrix size is $(2^{m+1} - 2) \times (2^{2m+1} - 2^{m+1})$ and the mutual coherence is $\mu \leq \frac{2^{(m+1)/2}+2}{2^m}$.
- Zhou–Helleseth–Udaya sequences: The matrix size is $(q-1)\times(q-1)^2$ and the mutual coherence is $\mu \leq \frac{\sqrt{q}}{q-1}$.

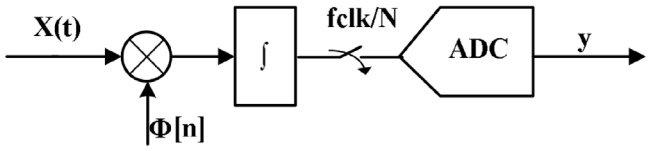

Fig. 11. CS transmitter block diagram [147].

The OMP is used in signal recovery. Simulation results show that the proposed matrices have better performance compared to the random Gaussian, random Bernoulli, random DFT, and the BCH matrices.

As an extension of the proposed matrix based on the photograph LDPC codes in [138], the authors in [143] constructed a new matrix to get rid of the performance degradation when increasing the compression rate N/M. The new design constructed a class of Extended Photograph LDPC Sparse Matrix (EPLDPC-SM), which proposes a better mutual coherence compared to the PLDPC-SM. The matrix requires low storage as its elements are $0, \pm 1$. With the aid of OMP, simulation results show that the performance of the proposed matrix is better than the PLDPC-SM, the random Gaussian matrix, and the random sparse binary matrix. Implementation is performed using shift registers as well.

The authors in [130] investigated a new approach to generate a measurement matrix suitable for adaptive BCS. The proposed Perceptual Variance Weight Matrix (PWM) is an adaptable measurement matrix based on variance of image blocks. The construction is performed by multiplying a binary random matrix with another constructed diagonal matrix whose elements are the variance calculated using $V_k = \frac{1}{b^2} \sum_{i=1}^{b} \sum_{j=1}^{b} (C_{i,j} - \mu)^2$, where b is the block size, $C_{i,j}$ is the coefficient of the image pixel in ith row and jth column, and μ is the mean of image coefficients. The resultant measurement matrix is a binary matrix of size MxN. DCT is used to transform the original signal into sparse domain and OMP is used for signal reconstruction. Simulation results show that the deployed algorithm is superior in image reconstruction quality compared to the normal BCS.

5. System implementation

Few papers have discussed the feasibility of implementing the CS system on physical hardware. Some papers contributed in implementing the transmitter blocks only. Others proposed using analog and digital circuits for implementing the full system. Listed below the contribution of each paper in implementing the system blocks.

5.1. CS transmitter implementation

Several papers in the literature [144–146] proposed an analog implementation for CS transmitter. As shown in Fig. 11, the proposed system implements the multiplication with Gaussian matrix using mixers, used as multipliers; FIR filters, used as integrators; and Successive Approximation Register Analog Digital Converter (SAR-ADC) for sampling. Allh building blocks used to implement the proposed circuit are analog components.

The work in [147] implements the CS transmitter using random filters. The original signal is convoluted with a random-tap FIR filter and the generated output is down-sampled to obtain the compressed signal. The authors mentioned the advantages of using random filters: maintaining the universality with various signals, requiring less storage and low computation complexity, and being time invariant and time localized. The paper mentioned that OMP and IHT are deployed in the recovery but did not give indication about the hardware implementation.

5.2. CS receiver implementation

Several papers in the literature proposed different architectures to implement the OMP. The authors in [148] were the first to propose a VLSI implementation for the OMP algorithm. The first step in Algorithm 1 is performed using 32-parallel multipliers to execute in single cycle. Step 6 is implemented using Alternative Cholesky Decomposition that does not require square root calculations for simplicity.

The work in [149] extended the work and replaced the Cholesky Decomposition with QR-Decomposition. The new approach solves the issue of the critical path due to the dot product operation. Simulation results show that the new architecture is 2.4 times faster than the state of art.

Another version of OMP entitled Matrix Inversion Bypass OMP (MIB-OMP) is implemented in [150] to reach high speed by sacrificing more area and power using parallelism. The design is synthesized on 65 nm CMOS.

The authors in [151] implemented CS reconstruction algorithm where part of the design is accelerated by implementing it as hardware on the FPGA and the other part is software model. A parallel matrix multiplication vector unit is used to accelerate the implemented hardware. Simulation results showed the effect of the use of hardware accelerators on the system speed.

5.3. CS full system implementation

CS is deployed in temperature and ECG sensors used in the WSN proposed in [152]. The implemented CS algorithm is deployed on WSN node using Laboratory Virtual Instrument Engineering Workbench (LAB VIEW) software. The compressed data is transmitted from the WSN node to the Gateway and reconstructed using a MATLAB® code calculating the RMSE. Simulation results show that 75% of data saving is achieved during the transmission.

The authors in [153] proposed a co-design of the CS system using Xilinx Zedboard FPGA. Random de-modulator is used in implementing the CS transmitter involving: multiplier, analog filter, and ADC. The chaotic random sequences are multiplied with the original signal, then passed through a low pass filter acting as integrator followed by an ADC with constant sampling rate to sample the signal in the analog domain. The compressed data is fed by the ARM Cortex to the reconstruction algorithm implemented on the Programmable Logic (PL) side. Simulation results show that the operating frequency is 61.21% lower than Nyquist frequency.

A similar design is proposed in [154] implementing the system on Xilinx Zedboard as well. The FPGA is connected to the PC where the data is fed into the implemented design using Ethernet cable. The ARM Cortex is used to run the software code and generate the chaotic sequences and pass them to the PL. Hardware accelerators for both matrix multiplication and IHT recovery algorithm are implemented in the PL side. Recovered signal through sigma-delta DAC is analyzed using an oscilloscope. Simulation results show that the operating frequency is 16% lower than Nyquist frequency.

6. Conclusion and future work

CS has proved itself as a possible replacement to Nyquist rate sampling criteria. This work provided a review on most of the performed work in the literature listing the contribution and the details of each paper. A fair comparison is performed with respect to the measurement matrix type, the matrix data entry type, the RIP support, the noise resilience, the memory cost, the encoding complexity, the decoding algorithm, and K and M relationship. The comparative study is performed from hardware perspective. It has been shown that binary measurement matrices are better than complex and float matrices with respect to memory cost. Satisfying either the RIP or the mutual incoherence is a mandatory condition for universality. Several metrics should be considered to ensure good performance of the reconstruction algorithm such as: the hardware complexity, which should be optimized along with the accuracy of signal recovery, which should be maximized. Being robust against noise effects is desirable as well.

Results show that 1-bit CS is the most appropriate CS type when targeting hardware friendly design due to its low memory cost. Deploying the 1-bit CS shall be beneficial in many applications such as WSNs and edge computing where sensor nodes have limited storage elements. The future road map shall involve implementing new reconstruction algorithms with better metrics than the literature to facilitate the physical implementation of the CS system and its deployment in applications.

Declaration of competing interest

There are no conflict of interest to declare.

Data availability

No data was used for the research described in the article

References

[1] H.J. Landau, Sampling, data transmission, and the nyquist rate, Proc. IEEE 55 (10) (1967) 1701–1706.
[2] D.L. Donoho, Compressed sensing, IEEE Trans. Inform. Theory 52 (4) (2006) 1289–1306.
[3] J. Song, Z. Liao, A new fast and parallel MRI framework based on contourlet and compressed sensing sensitivity encoding (CS-SENSE), in: International Conference on Machine Learning and Cybernetics, ICMLC, Jeju, South Korea, 2016, pp. 750–755.
[4] T. Minh-Chinh, N. Linh-Trung, T. Duc-Tan, On the implementation of chaotic compressed sensing for MRI, in: International Conference on Advanced Technologies for Communications, ATC, Hanoi, Vietnam, 2016, pp. 103–107.
[5] S. Kim, H. Ryu, Analysis and design of QAPM modulation using compressive sensing for low power communication, in: IEEE Military Communications Conference (MILCOM), Orlando, FL, USA, 2012.
[6] C. Zhang, J. Yu, Compressive sensing wireless channel modeling with digital map, IEEE Antennas Wirel. Propag. Lett. 12 (2013) 349–352.
[7] K. Yang, D.C. González, Y.C. Eldar, M. Médard, A sequence-based compressed sensing receiver for impulsive frequency shift keying, in: IEEE 23rd International Workshop on Signal Processing Advances in Wireless Communication (SPAWC), Oulu, Finland, 2022.
[8] S. Fujimura, R. Kamikawa, T. Konishi, Low-complexity coherent detection for short-reach links using compressed sensing and self-interference in optical OFDM subcarriers, in: 27th OptoElectronics and Communications Conference (OECC) and International Conference on Photonics in Switching and Computing (PSC), Toyama, Japan, 2022.
[9] Y. Xie, L. Fan, L. Yang, Y. Zhao, X. Hao, B. Dang, Depth- time dimension signal reconstruction of transient electromagnetic logging using compressed sensing, in: 4th International Conference on Intelligent Control, Measurement and Signal Processing, ICMSP, Hangzhou, China, 2022, pp. 255–258.
[10] K. Shetti, A. Vijayakumar, Evaluation of compressive sensing encoding on AR drone, in: Asia-Pacific Signal and Information Processing Association Annual Summit and Conference, APSIPA, Hong Kong, China, 2015, pp. 204–207.
[11] M. Balouchestani, Low-power wireless sensor network with compressed sensing theory, in: 4th Annual Caneus Fly By Wireless Workshop, Montreal, QC, Canada, 2011.
[12] V. Jagadeep, A. Rakesh, A. Karthikeyan, T. Shankar, Energy efficient transmission with mobile element using compressive sensing for wireless sensor network, in: International Conference on Innovations in Information, Embedded and Communication Systems (ICIIECS), Coimbatore, India, 2015.
[13] M. Balouchestani, K. Raahemifar, S. Krishnan, Low power Wireless Body Area networks with compressed sensing theory, in: IEEE 55th International Midwest Symposium on Circuits and Systems, MWSCAS, Boise, ID, USA, 2012, pp. 916–919.
[14] Y. Li, X. Cheng, Y. Zhang, W. Shi, J. Han, X. Zeng, A highly energy-efficient compressed sensing encoder with robust subthreshold clockless pipeline for wireless BANs, in: IEEE Biomedical Circuits and Systems Conference (BioCAS), Rotterdam, Netherlands, 2013, pp. 154–157.
[15] J.M.P. Nascimento, G. Martin, Hyperspectral compressive sensing on low energy consumption board, in: IEEE International Geoscience and Remote Sensing Symposium, IGARSS, Valencia, Spain, 2018, pp. 5065–5068.
[16] J. Akhtar, Space–time block codes and compressed sensing in spatially diverse radars, in: International Radar Conference, Lille, France, 2014.

[17] J. Akhtar, Compressed sensing for multistatic radar systems with arbitrary block codes, in: IEEE Radar Conference (RadarCon), Arlington, VA, USA, 2015, pp. 51–55.
[18] A. Focsa, M. Datcu, A. Anghel, Compressed sensing-based multi-aperture focusing of spaceborne transmitter/stationary receiver bistatic SAR data, in: IEEE Radar Conference (RadarConf20), Florence, Italy, 2020.
[19] C. Zheng, K. Liao, S. Ouyan, C. Li, Distributed computing method for synthetic aperture radar compressed sensing imaging based on MapReduce, in: IEEE 3rd International Conference on Electronic Information and Communication Technology, ICEICT, Shenzhen, China, 2021, pp. 541–544.
[20] J. Qian, D. Chen, W. Yan, FMCW SAR imaging based on compressed sensing, in: IEEE 3rd International Conference of Safe Production and Informatization, IICSPI, Chongqing City, China, 2021, pp. 287–290.
[21] N. Wang, X. Zhang, S. Wei, Y. Wu, J. Shi, High-resolution insar imaging via cs-based amplitude-phase separation algorithm, in: IEEE International Geoscience and Remote Sensing Symposium, Kuala Lumpur, Malaysia, 2022, pp. 915–918.
[22] Y. Wang, Q. Yang, Y. Zeng, B. Deng, H. Wang, Radar speech signal enhancement based on modified compressed sensing methods, in: 13th UK-Europe-China Workshop on Millimetre-Waves and Terahertz Technologies (UCMMT), Tianjin, China, 2020.
[23] Y. Hu, X. Zhang, S. Wei, Y. Ren, N. Wang, J. Shi, Adatomo-net: A novel deep learning approach for SAR tomography imaging and autofocusing, in: IEEE International Geoscience and Remote Sensing Symposium, 2022, Kuala Lumpur, Malaysia, 2022, pp. 587–590.
[24] S. Yi, X. Ji, G. Han, A method of SAS with sparse aperture based on compressive sensing, in: IEEE International Conference on Signal Processing, Communications and Computing (ICSPCC), Macau, China, 2020.
[25] W. Ning, A signal classification and recognition method based on over-complete dictionary in compressed sensing, in: IEEE 5th Information Technology and Mechatronics Engineering Conference, ITOEC, Chongqing, China, 2020, pp. 316–320.
[26] Lu Gan, Block compressed sensing of natural images, in: 15th International Conference on Digital Signal Processing, Cardiff, UK, 2007, pp. 403–406.
[27] P.T. Boufounos, R.G. Baraniuk, 1-bit compressive sensing, in: 42nd Annual Conference on Information Sciences and Systems, Princeton, NJ, 2008, pp. 16–21.
[28] A. Bourquard, F. Aguet, M. Unser, Optical imaging using binary sensors, Opt. Express 18 (2010) 4876–4888.
[29] H. Wang, Q. Wan, One bit support recovery, in: 6th International Conference on Wireless Communications Networking and Mobile Computing (WiCOM), Chengdu, China, 2010, pp. 1–4.
[30] Z. Wang, F. Liu, Y. Yin, B. Li, Y. Guo, Weighted L1-norm for one-bit compressed sensing based on approximated observation, in: IEEE MTT-S International Wireless Symposium (IWS), Shanghai, China, 2021.
[31] V. Ashok, T. Balakumaran, C. Gowrishankar, I.L.A. Vennila, A.N. Kumar, The fast haar wavelet transform for signal & image processing, Int. J. Comput. Sci. Inf. Secur., IJCSIS 7 (1) (2010) 126–130.
[32] A. Katharotiya1, S. Patel1, M. Goyani, Comparative analysis between DCT & DWT techniques of image compression, J. Inf. Eng. Appl. 1 (2) (2011) 9–17.
[33] A. Bhardwaj, R. Ali, Image compression using modified fast haar wavelet transform, World Appl. Sci. J. 7 (5) (2009) 647–653.
[34] Y.V. Balaso, S.S. Shinde, S.S. Tamboli, Image compression using modified fast haar wavelet transform, Int. J. Eng. Sci. Res. Technol. 5 (8) (2016) 141–147.
[35] A. Ghorpade, P. Katkar, Image compression using haar transform and modified fast haar wavelet transform, Int. J. Sci. Technol. Res. 3 (7) (2014).
[36] M. Du1, H. Zhao, C. Zhao, B. Li, The application of wavelet-based contourlet transform on compressed sensing, in: Communications Multimedia and Signal Processing, CMSP, Springer, Berlin, Heidelberg, 2012, p. 346.
[37] I. Sharif, S. Khare, Comparative analysis of haar and daubechies wavelet for hyper spectral image classification, in: International Archives of the Photogrammetry, Remote Sensing and Spatial Information Sciences, 2014, pp. 937–941.
[38] R. Monika, R. Hemalatha, S. Radha, Energy efficient weighted sampling matrix based CS technique for WSN, in: IEEE SENSORS, Busan, South Korea, 2015.
[39] B. Zhang, Y. Liu, J. Zhuang, L. Yang, A novel block compressed sensing based on matrix permutation, in: Visual Communications and Image Processing (VCIP), Chengdu, China, 2016.
[40] Z. Wang, S. Chen, Performance comparison of image block compressive sensing based on chaotic sensing matrix using different basis matrices, in: 2nd International Conference on Image, Vision and Computing, ICIVC, Chengdu, China, 2017, pp. 620–623.
[41] R. Zhang, C. Meng, C. Wang, Q. Wang, Compressed sensing reconstruction for wideband LFM signal based on fractional Fourier transform, in: International Conference on Big Data & Artificial Intelligence & Software Engineering, ICBASE, Bangkok, Thailand, 2021, pp. 132–135.
[42] S. Mun, J.E. Fowler, DPCM for quantized block-based compressed sensing of images, in: Proceedings of the 20th European Signal Processing Conference, EUSIPCO, Bucharest, Romania, 2012, pp. 1424–1428.
[43] J. Zhang, D. Zhao, F. Jiang, Spatially directional predictive coding for block-based compressive sensing of natural images, in: IEEE International Conference on Image Processing, Melbourne, VIC, Australia, 2013, pp. 1021–1025.
[44] K.Q. Dinh, H.J. Shim, B. Jeon, Measurement coding for compressive imaging using a structural measuremnet matrix, in: IEEE International Conference on Image Processing, Melbourne, VIC, Australia, 2013, pp. 10–13.
[45] W.D. Leon-Salas, Encoding compressive sensing measurements with golomb-rice codes, in: IEEE International Symposium on Circuits and Systems, ISCAS, Lisbon, Portugal, 2015, pp. 2177–2180.
[46] H. Bi, C. Zhao, H. Bi, Y. Liu, N. Li, Digital watermarking based on interleaving extraction block compressed sensing in contourlet domain, in: 9th International Congress on Image and Signal Processing, BioMedical Engineering and Informatics (CISP-BMEI), Datong, China, 2017, pp. 766–770.
[47] H.-C. Huang, F.-C. Chang, Y.-H. Chen, P.-L. Chen, Reliable transmission with variable-sized block compressed sensing, in: IEEE 3rd Global Conference on Life Sciences and Technologies (LifeTech), Nara, Japan, 2021, pp. 423–424.
[48] H.-C. Huang, F.-C. Chang, Y.-Y. Lu, P.-L. Chen, Quadtree-based block compressed sensing for reliable transmission applications, in: IEEE 4th Global Conference on Life Sciences and Technologies (LifeTech), Osaka, Japan, 2022, pp. 456–459.
[49] T. Bianchi, V. Bioglio, E. Magli, Analysis of one-time random projections for privacy preserving compressed sensing, IEEE Trans. Inf. Forensics Secur. 11 (2) (2016) 313–327.
[50] G. Kuldeep, Q. Zhang, Energy concealment based compressive sensing encryption for perfect secrecy for IoT, in: IEEE Global Communications Conference (GLOBECOM), Taipei, Taiwan, 2021.
[51] J. Liang, D. Xiao, Y. Xiang, R. Doss, A compressed sensing based image compression-encryption coding scheme without auxiliary information transmission, in: IEEE International Conference on Communications, ICC, Seoul, Korea, 2022, pp. 5573–5578.
[52] A. Kashyap, A. Pramanik, S.P. Maity, On block compressed sensing far end reconstruction using OFDM, in: Third International Conference on Image Information Processing, ICIIP, Waknaghat, India, 2015, pp. 162–167.
[53] E.J. Candes, J. Romberg, T. Tao, Robust uncertainty principles: exact signal reconstruction from highly incomplete frequency information, IEEE Trans. Inform. Theory 52 (2) (2006) 489–509.
[54] J. Bourgain, S.J. Dilworth, K. Ford, S. Konyagin, D. Kutzarova, Explicit constructions of RIP matrices and related problems, Duke Math. J. 159 (1) (2011) 145–185.
[55] L.R. Welch, Lower bounds on the maximum cross correlation of signals, IEEE Trans. Inform. Theory 20 (3) (1974) 397–399.
[56] V. Chandar, A negative result concerning explicit matrices with the restricted isometry property, 2008, Preprint.
[57] R. Berinde, A.C. Gilbert, P. Indyk, H. Karloff, M.J. Strauss, Combining geometry and combinatorics: A unified approach to sparse signal recovery, in: 46th Annual Allerton Conference on Communication, Control, and Computing, Urbana-Champaign, IL, USA, 2008, pp. 798–805.
[58] R. Berinde, P. Indyk, Sparse recovery using sparse random matrices, in: A. López-Ortiz (Ed.), LATIN 2010: Theoretical Informatics. LATIN 2010, in: Lecture Notes in Computer Science, vol. 6034, Springer, Berlin, Heidelberg.
[59] R. Baraniuk, M. Davenport, R. DeVore, M. Wakin, A simple proof of the restricted isometry property for random matrices, Constr. Approx. 28 (2008) 253–263.
[60] Z. Xu, Deterministic sampling of sparse trigonometric polynomials, J. Complexity 27 (2) (2011) 133–140.
[61] R. Calderbank, S. Howard, S. Jafarpour, Construction of a large class of deterministic sensing matrices that satisfy a statistical isometry property, IEEE J. Sel. Top. Sign. Proces. 4 (2) (2010) 358–374.
[62] S. Howard, R. Calderbank, S. Searle, A fast reconstruction algorithm for deterministic compressive sensing using second order ReedMuller codes, in: 42nd Annual Conference on Information Sciences and Systems, Princeton, NJ, USA, 2008, pp. 11–15.
[63] L. Applebaum, S.D. Howard, S. Searle, R. Calderbank, Chirp sensing codes: Deterministic compressed sensing measurements for fast recovery, Appl. Comput. Harmon. Anal. 26 (2) (2009) 283–290.
[64] L. Yu, J.P. Barbot, G. Zheng, H. Sun, Compressive sensing with chaotic sequence, IEEE Signal Process. Lett. 17 (8) (2010) 731–734.
[65] K. Li, C. Ling, L. Gan, Deterministic compressed-sensing matrices: Where toeplitz meets golay, in: IEEE International Conference on Acoustics, Speech and Signal Processing, ICASSP, Prague, Czech Republic, 2011, pp. 3748–3751.
[66] J. Zhang, J. Geng, Y. Lin, A.A. Wu, Low memory-cost scramble methods for constructing deterministic CS matrix, in: IEEE Workshop on Signal Processing Systems (SiPS), Hangzhou, China, 2015.
[67] A. Movahed, A. Panahi, G. Durisi, A robust RFPI-based 1-bit compressive sensing reconstruction algorithm, in: IEEE Information Theory Workshop, Lausanne, Switzerland, 2012, pp. 567–571.
[68] P.T. Boufounos, Greedy sparse signal reconstruction from sign measurements, in: Conference Record of the Forty-Third Asilomar Conference on Signals, Systems and Computers, Pacific Grove, CA, USA, 2009, pp. 1305–1309.
[69] W. Tang, W. Xu, X. Zhang, J. Lin, Recovery methods for 1-bit compressed sensing based on hamming distance, in: 3rd IEEE International Conference on Computer and Communications, ICCC, Chengdu, China, 2017, pp. 1362–1366.
[70] J. Tropp, A. Gilbert, Signal recovery from partial information via orthogonal matching pursuit, IEEE Trans. Inform. Theory 15 (2005).

[71] D.L. Donoho, Y. Tsaig, I. Drori, J. Starck, Sparse solution of underdetermined systems of linear equations by stagewise orthogonal matching pursuit, IEEE Trans. Inform. Theory 58 (2) (2012) 1094–1121.
[72] W. Dai, O. Milenkovic, Subspace pursuit for compressive sensing signal reconstruction, IEEE Trans. Inform. Theory 55 (5) (2009) 2230–2249.
[73] D. Needell, J.A. Tropp, CoSaMP: Iterative signal recovery from incomplete and inaccurate samples, Appl. Comput. Harmon. Anal. 26 (3) (2009) 301–331.
[74] R. Giryes, M. Elad, Cosamp and SP for the cosparse analysis model, in: Proceedings of the 20th European Signal Processing Conference, EUSIPCO, Bucharest, Romania, 2012, pp. 964–968.
[75] Y. Gaur, V.K. Chakka, Performance comparison of OMP and CoSaMP based channel estimation in AF-TWRN scenario, in: Third International Conference on Computer and Communication Technology, Allahabad, India, 2012, pp. 186–190.
[76] T. Blumensath, M.E. Davies, Iterative hard thresholding for compressed sensing, Appl. Comput. Harmon. Anal. 27 (3) (2009) 265–274.
[77] T.T. Do, L. Gan, N. Nguyen, T.D. Tran, Sparsity adaptive matching pursuit algorithm for practical compressed sensing, in: 42nd Asilomar Conference on Signals, Systems and Computers, Pacific Grove, CA, 2008, pp. 581–587.
[78] Z. Wei, J. Zhang, Z. Xu, Y. Huang, Y. Liu, X. Fan, Gradient Projection with Approximate L0 Norm Minimization for Sparse Reconstruction in Compressed Sensing, Multidisciplinary Digital Publishing Institute, 2018.
[79] S.S. Chen, D.L. Donoho, M.A. Saunders, Atomic decomposition by basis pursuit, Soc. Ind. Appl. Math. 43 (1) (2001) 129–159.
[80] L. Wang, X. Yin, H. Yue, J. Xiang, A Regularized Weighted Smoothed L0 Norm Minimization Method for Underdetermined Blind Source Separation, Multidisciplinary Digital Publishing Institute, 2018.
[81] J. Tropp, A. Gilbert, Signal recovery from random measurements via orthogonal matching pursuit, IEEE Trans. Inform. Theory 15 (2008) 4655–4666.
[82] S. Mun, J.E. Fowler, Block compressed sensing of images using directional transforms, in: Data Compression Conference, Snowbird, UT, USA, 2010, p. 547.
[83] M. Trocan, T. Maugey, J.E. Fowler, B. Pesquet-Popescu, Disparity-compensated compressed-sensing reconstruction for multiview images, in: IEEE International Conference on Multimedia and Expo, Singapore, 2010, pp. 1225–1229.
[84] J.E. Fowler, S. Mun, E.W. Tramel, Multiscale block compressed sensing with smoothed projected landweber reconstruction, in: 19th European Signal Processing Conference, Barcelona, Spain, 2011, pp. 564–568.
[85] S. Mun, J.E. Fowler, Residual reconstruction for block-based compressed sensing of video, in: Data Compression Conference, Snowbird, UT, USA, 2011, pp. 183–192.
[86] C. Chen, E.W. Tramel, J.E. Fowler, Compressed-sensing recovery of images and video using multihypothesis predictions, in: Conference Record of the Forty Fifth Asilomar Conference on Signals, Systems and Computers, ASILOMAR, Pacific Grove, CA, USA, 2011, pp. 1193–1198.
[87] Y. Hou, Y. Zhang, Effective hyperspectral image block compressed sensing using thress-dimensional wavelet transform, in: IEEE Geoscience and Remote Sensing Symposium, Quebec City, QC, Canada, 2014, pp. 2973–2976.
[88] A. Pramanik, S.P. Maity, DPCM-quantized block-based compressed sensing of images using robbins monro approach, in: IEEE International WIE Conference on Electrical and Computer Engineering (WIECON-ECE), Dhaka, Bangladesh, 2015, pp. 18–21.
[89] X. Jieqiong, C.R. del-Blanco, C. Cuevas, N. García, Fast image decoding for block compressed sensing based encoding by using a modified smooth l0-norm, in: IEEE 6th International Conference on Consumer Electronics - Berlin (ICCE-Berlin), Berlin, Germany, 2016, pp. 234–236.
[90] E. Candes, J. Romberg, Sparsity and incoherence in compressive sampling, Inverse Problems 23 (3) (2007) 969–985.
[91] W.U. Bajwa, J.D. Haupt, G.M. Raz, S.J. Wright, R.D. Nowak, Toeplitz-structured compressed sensing matrices, in: IEEE/SP 14th Workshop on Statistical Signal Processing, Madison, WI, USA, 2007, pp. 294–298.
[92] P. Indyk, Explicit constructions for compressed sensing of sparse signals, in: Proceedings of ACM-SIAM Symposium on Discrete Algorithms, 2008, 2008, pp. 30–33.
[93] J. Romberg, Compressive sensing by random convolution, SIAM J. Imaging Sci. 2 (4) (2009) 1098–1128.
[94] K. Li, C. Ling, L. Gan, Statistical restricted isometry property of orthogonal symmetric toeplitz matrices, in: IEEE Information Theory Workshop, Taormina, Italy, 2009, pp. 183–187.
[95] J. Haupt, L. Applebaum, R. Nowak, On the restricted isometry of deterministically subsampled Fourier matrices, in: 44th Annual Conference on Information Sciences and Systems (CISS), Princeton, NJ, USA, 2010.
[96] G. Zhang, S. Jiao, X. Xu, L. Wang, Compressed sensing and reconstruction with bernoulli matrices, in: IEEE International Conference on Information and Automation, Harbin, China, 2010, pp. 455–460.
[97] G. Zhang, S. Jiao, X. Xu, Compressed sensing and reconstruction with semi-Hadamard matrices, in: 2nd International Conference on Signal Processing Systems, Dalian, China, 2010, pp. 194–197.
[98] R.A. DeVore, Deterministic constructions of compressed sensing matrices, J. Complexity 23 (2007) 918–925.
[99] T.T. Do, T.D. Tran, L. Gan, Fast compressive sampling with structurally random matrices, in: IEEE International Conference on Acoustics, Speech and Signal Processing, Las Vegas, NV, USA, 2008, pp. 3369–3372.
[100] F. Sebert, Y.M. Zou, L. Ying, Toeplitz block matrices in compressed sensing and their applications in imaging, in: International Conference on Information Technology and Applications in Biomedicine, Shenzhen, China, 2008, pp. 47–50.
[101] L. Gan, T.T. Do, T.D. Tran, Fast compressive imaging using scrambled block Hadamard ensemble, in: 16th European Signal Processing Conference, Lausanne, Switzerland, 2008.
[102] T.T. Do, L. Gan, Y. Chen, N. Nguyen, T.D. Tran, Fast and efficient dimensionality reduction using structurally random matrices, in: IEEE International Conference on Acoustics, Speech and Signal Processing, Taipei, Taiwan, 2009, pp. 1821–1824.
[103] N.Y. Yu, Deterministic compressed sensing matrices from multiplicative character sequences, in: 45th Annual Conference on Information Sciences and Systems, Baltimore, MD, USA, 2011.
[104] N.Y. Yu, Additive character sequences with small alphabets for compressed sensing matrices, in: IEEE International Conference on Acoustics, Speech and Signal Processing, ICASSP, Prague, Czech Republic, 2011, pp. 2932–2935.
[105] X. Li, R. Zhao, S. Hu, Blocked polynomial deterministic matrix for compressed sensing, in: 6th International Conference on Wireless Communications Networking and Mobile Computing (WiCOM), Chengdu, China, 2010.
[106] Z. He, T. Ogawa, M. Haseyama, The simplest measurement matrix for compressed sensing of natural images, in: IEEE International Conference on Image Processing, Hong Kong, China, 2010, pp. 4301–4304.
[107] A. Amini, F. Marvasti, Deterministic construction of binary, bipolar, and ternary compressed sensing matrices, IEEE Trans. Inform. Theory 57 (4) (2011) 2360–2370.
[108] A. Amini, V. Montazerhodjat, F. Marvasti, Matrices with small coherence using p-ary block codes, IEEE Trans. Signal Process. 60 (1) (2012) 172–181.
[109] S. Li, F. Gao, G. Ge, S. Zhang, Deterministic construction of compressed sensing matrices via algebraic curves, IEEE Trans. Inform. Theory 58 (8) (2012) 5035–5041.
[110] L. Gan, K. Li, C. Ling, Golay meets Hadamard: Golay-paired Hadamard matrices for fast compressed sensing, in: IEEE Information Theory Workshop, Lausanne, Switzerland, 2012, pp. 637–641.
[111] Y. Wang, Z. Tian, C. Feng, S. Feng, P. Zhang, Performance analysis of generalized block diagonal structured random matrices in compressive sensing, in: International Symposium on Communications and Information Technologies, ISCIT, Gold Coast, QLD, Australia, 2012, pp. 793–797.
[112] X. Liu, S. Xia, Constructions of quasi-cyclic measurement matrices based on array codes, in: IEEE International Symposium on Information Theory, Istanbul, Turkey, 2013, pp. 479–483.
[113] N.Y. Yu, N. Zhao, Deterministic construction of real-valued ternary sensing matrices using optical orthogonal codes, IEEE Signal Process. Lett. 20 (11) (2013) 1106–1109.
[114] M.M. Mohades, A. Mohades, A. Tadaion, A Reed–Solomon code based measurement matrix with small coherence, IEEE Signal Process. Lett. 21 (7) (2014) 839–843.
[115] S. Li, G. Ge, Deterministic construction of sparse sensing matrices via finite geometry, IEEE Trans. Signal Process. 62 (11) (2014) 2850–2859.
[116] X. Jiang, Z. Xie, Sparse binary matrixes of QC-LDPC code for compressed sensing, in: 11th International Computer Conference on Wavelet Actiev Media Technology and Information Processing, ICCWAMTIP, Chengdu, China, 2014, pp. 284–288.
[117] F. Fan, Toeplitz-structured measurement matrix construction for chaotic compressive sensing, in: Fifth International Conference on Intelligent Control and Information Processing, Dalian, China, 2015, pp. 19–22.
[118] A. Amini, H. Bagh-Sheikhi, F. Marvasti, From paley graphs to deterministic sensing matrices with real-valued gramians, in: International Conference on Sampling Theory and Applications (SampTA), Washington, DC, USA, 2015, pp. 372–376.
[119] A. Ravelomanantsoa, H. Rabah, A. Rouane, Compressed sensing: A simple deterministic measurement matrix and a fast recovery algorithm, IEEE Trans. Instrum. Meas. 64 (12) (2015) 3405–3413.
[120] R.R. Naidu, P. Jampana, C.S. Sastry, Deterministic compressed sensing matrices: Construction via Euler squares and applications, IEEE Trans. Signal Process. 64 (14) (2016) 3566–3575.
[121] P. Sasmal, R.R. Naidu, C.S. Sastry, P. Jampana, Composition of binary compressed sensing matrices, IEEE Signal Process. Lett. 23 (8) (2016) 1096–1100.
[122] M. Elad, Optimized projections for compressed sensing, IEEE Trans. Signal Process. 55 (12) (2007) 5695–5702.
[123] W. Chen, M.R.D. Rodrigues, I.J. Wassell, Projection design for statistical compressive sensing: A tight frame based approach, IEEE Trans. Signal Process. 61 (8) (2013) 2016–2029.
[124] S. Hsieh, C. Lu, S. Pei, Compressive sensing matrix design for fast encoding and decoding via sparse FFT, IEEE Signal Process. Lett. 25 (4) (2018) 591–595.
[125] A. Averbuch, S. Dekel, S. Deutsch, Adaptive compressed image sensing using dictionaries, SIAM J. Imaging Sci. 5 (1) (2012) 57–89.

[126] L. Haiqiang, Y. Jihang, H. Gang, Y. Hongsheng, Z. Aichun, Deterministic construction of measurement matrices based on bose balanced incomplete block designs, IEEE Access 6 (2018) 21710–21718.
[127] Z. Gu, Z. Zhou, Y. Yang, A.R. Adhikary, X. Cai, Deterministic compressed sensing matrices from sequences with optimal correlation, IEEE Access 7 (2019) 16704–16710.
[128] W. Yina, S. Morganb, J. Yangc, Y. Zhang, Practical compressive sensing with toeplitz and circulant matrices, Proc. SPIE - Int. Soc. Opt. Eng. 7744 (2010).
[129] S. Li, G. Ge, Deterministic sensing matrices arising from near orthogonal systems, IEEE Trans. Inform. Theory 60 (4) (2014) 2291–2302.
[130] R. Monika, R. Senthil, R. Narayanamoorthi, S. Dhanalakshmi, Perceptual variance weight matrix based adaptive block compressed sensing for marine image compression, in: OCEANS, Chennai, India, 2022.
[131] N. Linh-Trung, D. Van Phong, Z.M. Hussain, H.T. Huynh, V.L. Morgan, J.C. Gore, Compressed sensing using chaos filters, in: Australasian Telecommunication Networks and Applications Conference, Adelaide, SA, Australia, 2008, pp. 219–223.
[132] M.A.T. Figueiredo, R.D. Nowak, S.J. Wright, Gradient projection for sparse reconstruction: Application to compressed sensing and other inverse problems, IEEE J. Sel. Top. Sign. Proces. 1 (4) (2007) 586–597.
[133] H.L. Yap, A. Eftekhari, M.B. Wakin, C.J. Rozell, The restricted isometry property for block diagonal matrices, in: 45th Annual Conference on Information Sciences and Systems, Baltimore, MD, USA, 2011.
[134] A.G. Dimakis, R. Smarandache, P.O. Vontobel, LDPC codes for compressed sensing, IEEE Trans. Inform. Theory 58 (5) (2012) 3093–3114.
[135] Z. Wen, W. Yin, H. Zhang, D. Goldfarb, On the convergence of an active set method for l1-minimization, Optim. Methods Softw. 27 (6) (2011) 1–20.
[136] L. Bingjie, Y. Meng, K. Guangxing, Z. Mingfa, The minimax method of design of measurement matrices for compressed sensing based on incoherence criterion, in: Fifth International Conference on Intelligent Computation Technology and Automation, Zhangjiajie, Hunan, China, 2012, pp. 352–355.
[137] V. Abrol, P. Sharma, S. Budhiraja, Deterministic compressed-sensing matrix from grassmannian matrix: Application to speech processing, in: 3rd IEEE International Advance Computing Conference, IACC, Ghaziabad, India, 2013, pp. 1165–1170.
[138] J. Zhang, G. Han, Y. Fang, Deterministic construction of compressed sensing matrices from protograph LDPC codes, IEEE Signal Process. Lett. 22 (11) (2015) 1960–1964.
[139] E.J. Candes, T. Tao, Near-optimal signal recovery from random projections: Universal encoding strategies? IEEE Trans. Inform. Theory 52 (12) (2006) 5406–5425.
[140] Z. Li, J. Xie, G. Zhu, X. Peng, Y. Xie, Y. Choi, Block-based projection matrix design for compressed sensing, Chin. J. Electron. 25 (3) (2016) 551–555.
[141] S. Becker, J. Bobin, E.J. Cands, Nesta: A fast and accurate firstorder method for sparse recovery, SIAM J. Imaging Sci. 4 (1) (2009).
[142] R. Berinde, P. Indyk, Sparse recovery using sparse random matrices. [Online]. Available: http://people.csail.mit.edu/indyk/report.pdf.
[143] K. Chen, Y. Fang, G. Cai, J. Zhang, G. Han, P. Chen, Constructions of flexible-size deterministic measurement matrices using protograph LDPC codes and Hadamard codes, in: IEEE 91st Vehicular Technology Conference (VTC2020-Spring), Antwerp, Belgium, 2020.
[144] X. Chen, Z. Yu, S. Hoyos, B.M. Sadler, J. Silva-Martinez, A sub-nyquist rate sampling receiver exploiting compressive sensing, IEEE Trans. Circuits Syst. I. Regul. Pap. 58 (3) (2011) 507–520.
[145] P. Bahmanyar, S. Hosseini-Khayat, Design of a low-power compressive sampling circuit for Gaussian sensing matrices, in: 21st Iranian Conference on Electrical Engineering (ICEE), Mashhad, Iran, 2013.
[146] H. Lange, S. Schmale, D. Peters-Drolshagen, S. Paul, Comparison of implementation and recovery for 'multi channel compressed sensing, in: IEEE International Symposium on Circuits and Systems (ISCAS), Florence, Italy, 2018.
[147] J.A. Tropp, M.B. Wakin, M.F. Duarte, D. Baron, R.G. Baraniuk, Random filters for compressive sampling and reconstruction, in: 2006 IEEE International Conference on Acoustics Speech and Signal Processing Proceedings, Toulouse, France, 2006.
[148] A. Septimus, R. Steinberg, Compressive sampling hardware reconstruction, in: Proceedings of 2010 IEEE International Symposium on Circuits and Systems, Paris, France, 2010, pp. 3316–3319.
[149] J.L.V.M. Stanislaus, T. Mohsenin, High performance compressive sensing reconstruction hardware with QRD process, in: IEEE International Symposium on Circuits and Systems, ISCAS, Seoul, South Korea, 2012, pp. 29–32.
[150] G. Huang, L. Wang, High-speed signal reconstruction with orthogonal matching pursuit via matrix inversion bypass, in: IEEE Workshop on Signal Processing Systems, Quebec City, QC, Canada, 2012, pp. 191–196.
[151] G. Li, J. Gu, Q. Song, Y. Lu, B. Zhou, The hardware design and implementation of a signal reconstruction algorithm based on compressed sensing, in: Fifth International Conference on Intelligent Networks and Intelligent Systems, Tianjin, China, 2012, pp. 96–100.
[152] P. Chakraborty, C. Tharini, M. Abidha, Hardware implementation of compressed sensing algorithm, in: International Conference on Recent Trends in Electrical, Control and Communication, RTECC, Malaysia, Malaysia, 2018, pp. 46–50.
[153] M.L. Acosta, L. De Micco, Xampling and chaotic compressive sensing signal acquisition and reconstruction system, in: XVII Workshop on Information Processing and Control (RPIC), Mar Del Plata, Argentina, 2017.
[154] M.L. Acosta, M. Antonelli, L. De Micco, Chaotic compressed sensing system for 16x sub-nyquist signal reconstruction, in: Argentine Conference on Electronics, CAE, Mar del Plata, Argentina, 2019, pp. 31–36.

Sherif Hosny received the B.Sc. (Hons.) and M.Sc. degrees in electronics and computer engineering from Cairo University, Cairo, Egypt, in 2014 and 2018, respectively, and currently working on the Ph.D. degree in computer engineering at Ain Shams University. He is currently a staff integration and verification engineer at STMicroelectronics, Cairo, Egypt. His research interests include Systems-on-Chip (SoC), Field Programmable Gate Array (FPGA), Software Defined Radio (SDR), digital verification, and compressed sensing. He has published 6 articles in refereed international journals and conferences.

M. Watheq El-kharashi received the B.Sc. (Hons.) and M.Sc. degrees in computer engineering from Ain Shams University, Cairo, Egypt, in 1992 and 1996, respectively, and the Ph.D. degree in computer engineering from the University of Victoria, Victoria, BC, Canada, in 2002. He is currently a Professor of computer organization and a chair of the Department of Computer and Systems Engineering. Ain Shams University; and also an Adjunct Professor with the Department of Electrical and Computer Engineering, University of Victoria. He has published 170 articles in refereed international journals and conferences and authored two books and eight book chapters.

His current research interests include advanced system architectures, especially Networks-on-Chip (NoC), Systems-on-Chip (SoC), and secure hardware. More specific interests include hardware architectures for networking (network processing units) and security; advanced microprocessor design, simulation, performance evaluation, and testability; and computer architecture and computer networks education.

Amr T. Abdel-Hamid is an entrepreneur and an Associate Professor of Electronics/Networks Departments (Duel Appointed) at both the German University in Cairo (GUC) since 2006 and German International University — Berlin since 2023. He is also serving as the Vice Dean of Student affairs in the Faculty of Information Engineering and Technology at the GUC. His fields of experience span from hard core technology disciplines like hardware verification to cutting edge technologies such as Internet-of things (IOT) and AIOT solution design. Amr got both his Ph.D. and Ma.Sc. in Computer Engineering from Concordia University, Montreal, Canada at 2005, and 2001 respectively, as well as his B.Sc. from Cairo University at 1997. He got more than 50 refereed publications and more than 250 student projects supervised. Amr served as a judge and a consultant in many conferences, organizations, and competitions such as TIEC, ITIDA, NewCas Conference, ICM Conference and IEEE Journal of Circuits and Systems.

As an entrepreneur, Amr founded SSTM Egypt at 2016, where he still serving as the managing director of the company. SSTM is a leader in transforming revolutionary ideas into products that can be rapidly dispatched in your home and office. Its mission has always been designing and developing innovative products and systems to improve the quality of life. Amr leads the design team of SSTM, where they designed and implemented many innovative IOT products, including IOTPia, IoTiK, CoolTeck, CaCiot, as well as many wireless connected customized smart solutions.